Stem Cell Reports
Article

OPEN ACCESS

Electrical Guidance of Human Stem Cells in the Rat Brain

Jun-Feng Feng,[1,2,3] Jing Liu,[4] Lei Zhang,[1] Ji-Yao Jiang,[2,3] Michael Russell,[5] Bruce G. Lyeth,[6] Jan A. Nolta,[4] and Min Zhao[1,*]

[1]Departments of Dermatology and Ophthalmology, Institute for Regenerative Cures, University of California Davis, 2921 Stockton Boulevard, Sacramento, CA 95817, USA
[2]Department of Neurosurgery, Ren Ji Hospital, School of Medicine, Shanghai Jiao Tong University, Shanghai 200127, People's Republic of China
[3]Shanghai Institute of Head Trauma, Shanghai 200127, People's Republic of China
[4]Stem Cell Program and Institute for Regenerative Cures, University of California Davis, Sacramento, CA 95817, USA
[5]Aaken Laboratories, Davis, CA 95616, USA
[6]Department of Neurological Surgery, University of California Davis, Davis, CA 95616, USA
*Correspondence: minzhao@ucdavis.edu
http://dx.doi.org/10.1016/j.stemcr.2017.05.035

SUMMARY

Limited migration of neural stem cells in adult brain is a roadblock for the use of stem cell therapies to treat brain diseases and injuries. Here, we report a strategy that mobilizes and guides migration of stem cells in the brain *in vivo*. We developed a safe stimulation paradigm to deliver directional currents in the brain. Tracking cells expressing GFP demonstrated electrical mobilization and guidance of migration of human neural stem cells, even against co-existing intrinsic cues in the rostral migration stream. Transplanted cells were observed at 3 weeks and 4 months after stimulation in areas guided by the stimulation currents, and with indications of differentiation. Electrical stimulation thus may provide a potential approach to facilitate brain stem cell therapies.

INTRODUCTION

Neural stem cells/progenitor cells (NSCs) promise great hope for various neurological diseases. Researchers have demonstrated that NSCs are able to migrate and differentiate into adult rat brain and spinal cord (Flax et al., 1998; Snyder and Teng, 2012; Tabar et al., 2005). The human brain, however, poses a particular challenge for migrating NSCs or neuroblasts due to our larger brain size and the distances that cells must travel. Endogenous neuroblasts reside in the subventricular zone (SVZ) and hippocampus, deep in the brain. Neuroblasts from these niches have to migrate long distances to reach lesions in the cortex or other extra-hippocampal regions. Another hurdle is that transplanted NSCs have very poor motility due to suppression of migration by NSCs to each other and their progenies (Ladewig et al., 2014). Expanding the limits of migration of stem cells in brain is therefore a key step in stem cell therapies for the human brain (Trounson and McDonald, 2015). We aim to develop techniques that can mobilize and guide stem cells in the brain *in vivo*, which has not yet been achieved.

We chose the rostral migration stream (RMS) to develop our stimulation technique because this is one of the most active migratory paths in the brain, and its cellular and molecular mechanisms are well understood (Anton et al., 2004; Curtis et al., 2007; Mobley and McCarty, 2011; Sanai et al., 2011; Staquicini et al., 2009). Newly born neuroblasts and transplanted hNSCs placed at the SVZ normally migrate directionally downstream to the olfactory bulb (OB), guided by various cues, including multiple chemical gradients and flow of cerebral spinal fluid (Flax et al., 1998; Sawamoto et al., 2006; Snyder and Teng, 2012; Tabar et al., 2005; Wu et al., 1999). This model allows us to test whether our technique is able to guide hNSCs to travel upstream toward the lateral ventricle (LV) region on the ipsilateral side, against endogenous directional cues.

Electric fields (EFs) provide a powerful signal with which to stimulate and guide migration of many types of cells *in vitro*, including NSCs (Cao et al., 2013; Feng et al., 2012a; Li et al., 2008; Meng et al., 2011; Yao et al., 2008, 2009; Zhao et al., 2006). Normally, weak EFs in the brain may aid in guiding the migration of neuroblasts from the SVZ to the OB (Cao et al., 2013). We hypothesized that a stronger applied EF would provide a signal sufficient to guide some of the hNSCs injected in the middle of the RMS to move upstream toward the SVZ, against the intrinsic guidance mechanisms (Figure 1).

RESULTS

The Overall Research Design

First, we transplant human neural stem cells (hNSCs) into the RMS (Figure 1A). The transplanted cells migrate to the OB, following the endogenous directional signal (Figure 1B). We then apply electric currents along the RMS with minimal effects on brain electrical activities and motor behavior (Figure 1C). If the EFs are applied against the endogenous direction of neuroblasts (i.e., downstream of the SVZ to the OB), and if the electrical guidance effect is strong enough, we should see transplanted cells being

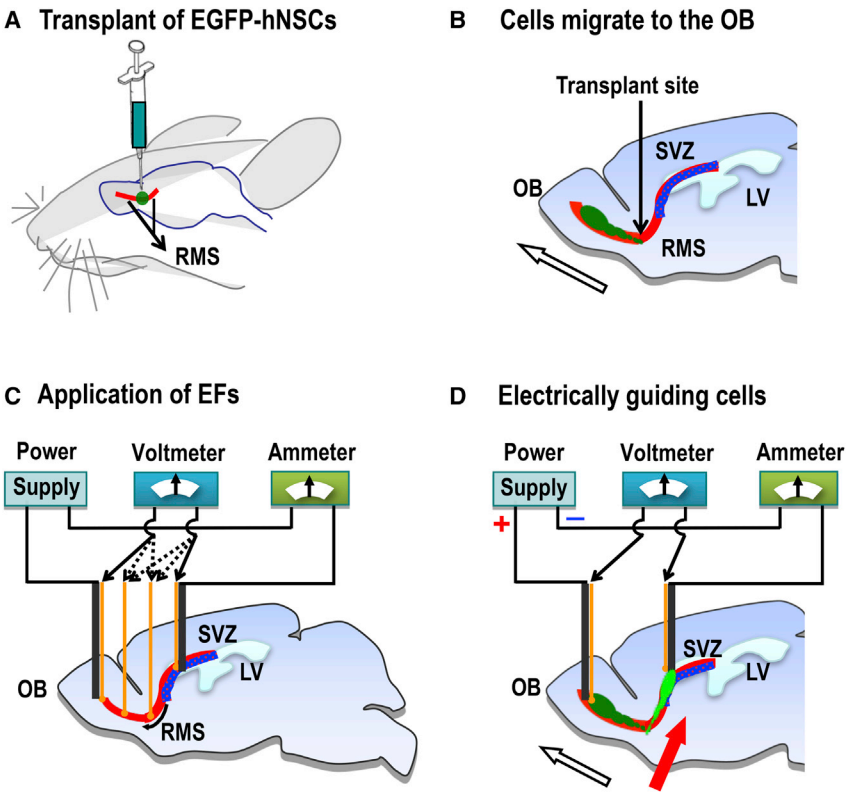

Figure 1. Experimental Design to Guide Migration of Human Neural Stem Cells in Rat Brain

(A) Transplantation of human neural stem cells (hNSCs) expressing EGFP (EGFP-hNSCs) (in green) at the middle of rostral migration stream (RMS, in red) in rat brain.

(B) Transplanted hNSCs migrate along the RMS toward the olfactory bulb (OB) (in dark green, migration direction indicated by white arrow). SVZ, subventricular zone (blue); LV, lateral ventricle.

(C) *In vivo* application of electrical stimulation and evaluations for its effectiveness, stability, and safety in rat brain. Ag/AgCl electrodes (yellow) for measurement. Carbon electrodes (black) for delivery of electric currents.

(D) Electrically guiding migration of transplanted hNSCs to SVZ (in bright green, migration direction indicated by red arrow).

guided to migrate against the endogenous cues and upstream to the SVZ (Figure 1D).

To Track NSCs in the Brain, We First Developed an hNSC Line that Expresses EGFP

The previously described hNSCs from H9 (Feng et al., 2012a) were transduced with MNDU3-luciferase-PGK-EGFP, a lentiviral vector expressing EGFP. EGFP-positive cells enriched by cell sorting provided a consistent number of cells for transplantation (Figure S1). The transduced cells maintained markers for NSCs and allowed us to differentiate types of cells (Figures 2A–2D). We tested whether expression of EGFP altered galvanotaxis. Applied EFs effectively mobilized and guided the migration of the hNSCs expressing EGFP (EGFP-hNSCs) in the same way as their parental cells, and that of neuroblasts from neonatal rat brain and from the SVZ of adult mice (Figures 2E–2H and S2; Movie S1) (Cao et al., 2013; Feng et al., 2012a; Li et al., 2008).

We Then Optimized the Electrical Stimulation Scheme to Effectively Guide Cells

Our setup had a unique modification of the classic galvanotaxis chamber with a very small conductive volume (~20 μL) over a large surface area (400 mm^2), ensuring minimal electric currents at physiological voltages (less than 1 mA). This design efficiently dissipates heat generated and minimizes changes in ions and perturbation of culture conditions. Cells exposed to a field of 100–200 mV/mm remained healthy and motile for several days (Song et al., 2007). With this design, however, it was not possible to deliver direct current (DC) EFs to the brain, because the large conductive volume reduces resistance and allows currents of hundreds and thousands times higher to pass through the tissues at similar voltage, inducing a significant Joule effect, changes in pH and ion concentrations, and electrode by-products. We developed optimal stimulation schemes using intermittent EFs (iEFs) that minimized detrimental effects while maintaining effective guidance for migration of hNSCs. iEFs with specific on and off ratios showed significant guidance effects on directional migration of hNSCs while maintaining cell viability after prolonged stimulation (Figures S3A and S3B; Movies S2 and S3), and induced negligible changes in temperature and pH in the culture chamber (Figures S3C–S3E3).

Electrode Pairs Were Used to Simultaneously Deliver and Monitor Stable Currents at the Same Time

Based on the preliminary test, we chose carbon electrodes to deliver current and silver/silver chloride (Ag/AgCl) electrodes to monitor the EF induced (Figures 3B and S4A). Two configurations of electrodes were used: two plus four (2 + 4)

(Figure 3C), and two pairs (2 + 2) (Figure 3D). The 2 + 4 electrodes have more detailed measurement points. Paired electrodes were inserted and immobilized in the brain of anesthetized animals with a stereotactic frame. The electrical currents were delivered to the brain in animals under continuous anesthesia or in free-moving status after recovery from surgical anesthesia. After the rat head was immobilized in a stereotaxic stage, the electrodes were inserted into the brain from a window in the skull surgically made to expos the dura. The electrodes were fixed to a holder with a pre-determined depth and spacing that corresponded to the points along the RMS (Figures 3 and S4A). Histology sections confirmed that injection needle and electrodes were correctly placed and secured using stereotactic manipulation and electrode immobilization (Figures 4A, 4B, 4E, and 5A). Continuous monitoring of the EFs and currents in the brain during stimulation allowed adjustment to ensure stable voltage and currents in the brain (Figures S4B–S4E). During continuous anesthesia, the electric currents were delivered to the brain along the RMS for up to 10 hr (Figure 3D). For animals that recovered from anesthesia and moved freely in the cage, we developed a portable miniaturized stimulator with a button battery and a programmable chip to administer stimulation. The battery and programmable chip were housed in a transparent plastic tube. After stereotaxic electrode implantation, the battery-chip tube configuration was secured to the skull with dental acrylic (Figure 3E).

Electroencephalographic and Motor Functions Suggested Good Tolerance of the Rats to Surgery and Electrical Stimulation

No seizures were observed in any animals during or after the electrical stimulation. We placed two electroencephalogram (EEG) recording electrodes in the left and right frontal bone next to the dura, using a modified method described previously (Feng et al., 2012b) (Figures S5A and S5B). Electrical stimulation used in our experiments had negligible effects on the EEG. Post-stimulation recording showed waveforms similar to those pre-stimulation (Figure S5E). Quantitative analysis confirmed complete overlap of the EEG recorded from rat before stimulation and after intermittent EF stimulation (Figure S5D). Frequency dependence of the power analysis based on the harvested EEGs showed no statistically significant changes in theta or beta waves, but slightly increased the power of low gamma wave during iEF stimulation (Figure S5E).

To determine the effects of electrode implantation and stimulation on animal behavior, we recorded normal movement of the animals after recovery from anesthesia and for more than 3 weeks (Figure S5F). We evaluated the effects on locomotor function (Rotarod) and fine motor coordination function (horizontal ladder walk) (Hamm et al., 1994; Metz and Whishaw, 2002, 2009). The Rotarod performance of the cell transplantation group alone and the cell transplantation plus electrodes groups were essentially unchanged from baseline on all post-surgery test days. There appeared to be a weak trend for the cell transplantation with stimulation group to have a shorter duration on the Rotarod at day 1 compared with baseline, but differences were not statistically significant ($p = 0.33$, t test). The horizontal ladder walk performance of the cell transplantation group alone and the cell transplantation plus electrode groups were essentially unchanged from baseline on all post-surgery test days. There appeared to be a weak trend for the cell transplantation with stimulation group to have a greater number of foot slips on the ladder walk on day 1 compared with baseline, but differences were not statistically significant ($p = 0.32$, t test). These tests suggest that the surgery and stimulation did not induce significant alterations of motor function (Hamm et al., 1994; Metz and Whishaw, 2009; Stout et al., 2013).

We Stimulated and Guided Migration of hNSCs Transplanted into the Middle of the RMS

With no electrical stimulation (no electrode insertion control group, and electrode insertion with no electrical stimulation sham group), hNSCs transplanted into the middle of the RMS migrated uniformly toward the OB (Figures 4A and 4E), consistent with previous reports of migration of hNSCs toward the OB when transplanted in the SVZ (Flax et al., 1998; Tabar et al., 2005). These results confirmed the robust intrinsic guidance signals toward the OB. When an electrical stimulation was applied toward the LV (upstream of the RMS), significant numbers of cells were found near the ipsilateral LV region (Figures 4B and 4B″), which was not observed in any of the control and sham brains (Figures 4A″ and 4E″). Serial sections of the brain demonstrated consistent migration of hNSCs upstream toward the ipsilateral SVZ (Figure 4D). Co-staining with human SOX2 antibodies confirmed the undifferentiated status of the migrating hNSCs (Figure 4C). To exclude the possibility of electrode insertion as a cause of inducing migration of hNSCs toward the LV direction, we positioned electrodes the same way without switching on the field (sham group). No EGFP signals were observed around the electrode near the LV region (Figures 4E and 4E″). In brain sections with the injection sites with electrode positions visible, we counted the EGFP-positive cells and measured the distance between the transplant site and cells furthest in the OB direction, and in the LV direction. Following electrical stimulation, NSCs were observed upstream near the LV region. No NSCs were observed in the LV region in control group and sham

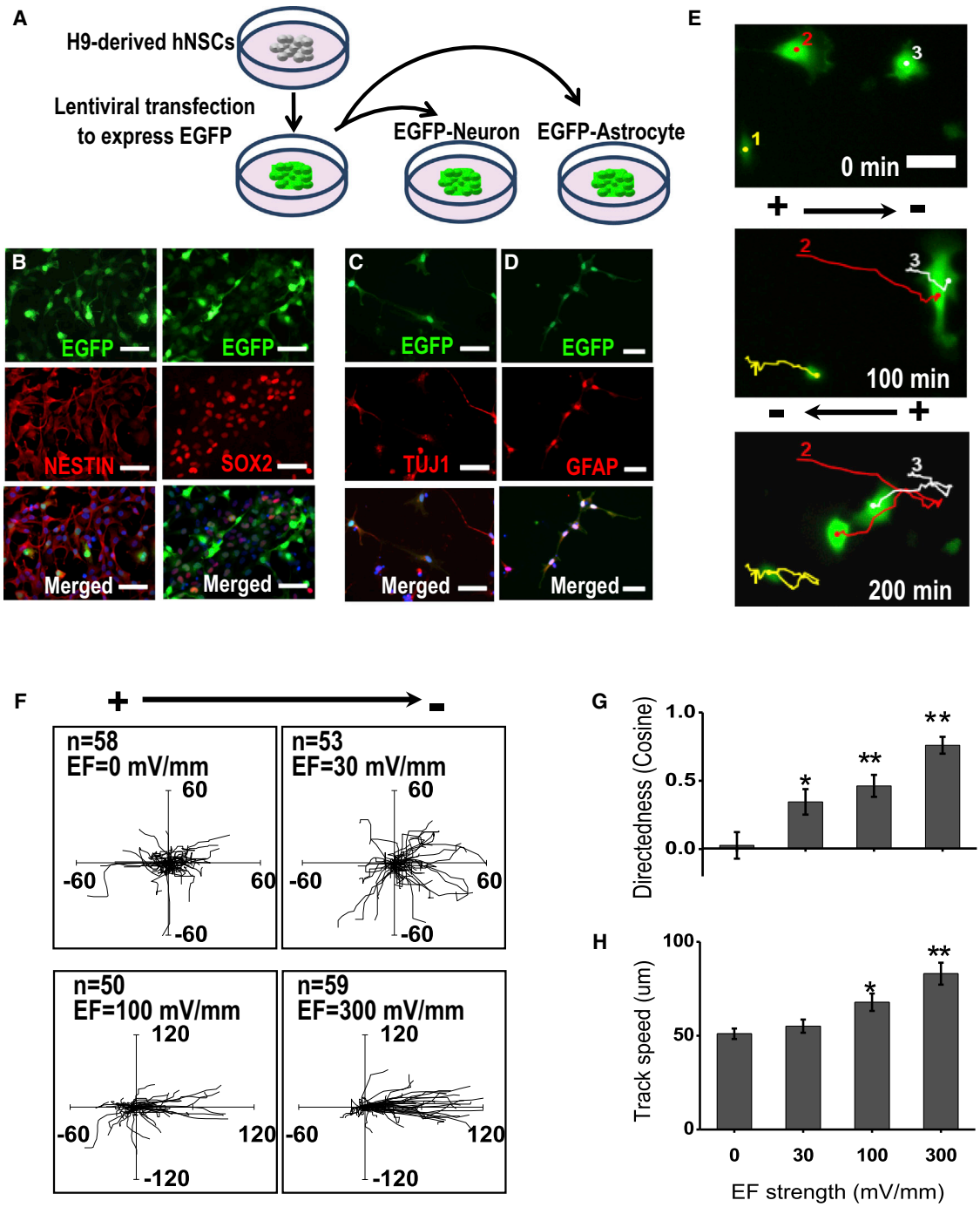

Figure 2. Electric Fields Stimulate and Guide Migration of EGFP-hNSCs

(A) Derivation of hNSCs expressing EGFP and verification of the pluripotent capacity. See also Figure S1 for details of derivation of hNSCs from human embryonic stem cells (hESCs, line H9) and the lentivirus used.

(B) Lentiviral transfected hNSCs stably expressing EGFP maintained the pluripotent markers of NESTIN and SOX2.

(C and D) The EGFP-hNSCs could be induced to differentiate into neuron marker TUJ1-positive cells (C) and astrocyte marker GFAP-positive cells (D). DAPI nuclear counterstains are blue.

(E–H) Lentiviral transfected hNSCs (EGFP-hNSCs, 1, 2, 3 are the typical ones) have the same electrotaxis response as parental cells. (E) Time-lapse images show robust cathodal migration of EGFP-hNSCs in an electric field (EF) (250 mV/mm). Reversal of the field polarity reversed the direction of cell migration. See also Movie S1. (F–H) Trajectories of cells with the starting point at the origin. Applied EFs as

(legend continued on next page)

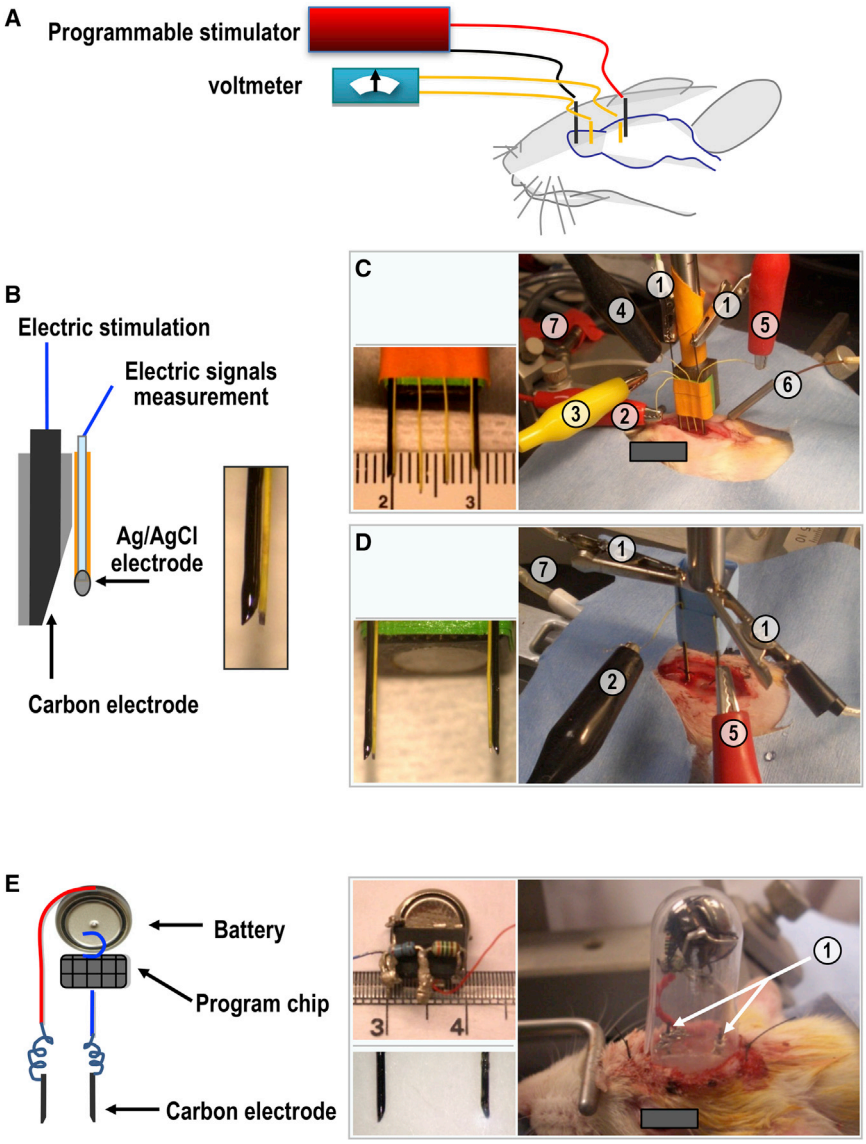

Figure 3. Implementation of Electrical Stimulation in Brain *In Vivo* in Anesthetized and Awake Free-Moving Animals

(A) Schematic of a power supply, electrodes, and a rat brain.

(B) Carbon electrodes and silver/silver chloride (Ag/AgCl) electrodes for *in vivo* current delivery and monitoring, respectively. See also Figure S4A for parameters in detail.

(C) Assembled electrodes (left) for electrical stimulation and parameter monitoring along the rostral migration stream (RMS) in the brain of an anesthetized rat with no cell transplantation (right). See Figures S5A and S5B.

(D) Assembled electrodes (left) for *in vivo* stimulation and monitoring for 10 hr started at 24 hr after EGFP-hNSCs transplantation (right).

(E) A stimulator that can be fixed on the skull of a rat, which allows the rat free movement after awaking from anesthesia. The stimulator can be remotely controlled through the programmable chip (on/off, wave form, and size and duration of the currents).

① Carbon electrodes connected to power supply for applying EF stimulation; ②, ③, ④, ⑤ Ag/AgCl electrodes connected to ammeter and/or voltmeter for measurement of the electric current and voltage; ⑥ probe in temporalis for brain temperature recording; ⑦ trachea cannula.

group (Figure 4F). Maximal migration distance of hNSCs upstream to the LV region was found to be the same as that to the OB when the electrical stimulation was applied to the direction of LV (Figure 4G).

The Guided Migration and Enhanced Cell Motility in the Brain Persisted Long after Stimulation

To determine longer-term cell survival, we examined serial sagittal sections of the rat brains 3 weeks and 4 months after electrical stimulation. Detailed examination of the serial brain sections revealed that NSCs migrated from the injection site to the LV region and to the contralateral hemisphere (Figure 5B). EGFP signals were detected further away from the transplant site even beyond the electrode in the posterior region of the SVZ, and in the corpus callosum of the contralateral hemisphere, which were not found in the control and sham brains (Figures 5 and S6). The migration of transplanted cells beyond the attractive electrode to

small as 30 mV/mm induced significant directional migration. The unit of the axes is micrometers. Voltage dependence of the directedness (G) and track speed (H). Field strength is as shown, and duration of the experiment is 1 hr.

Data are presented as mean ± SEM from three or more independent experiments. *$p < 0.05$, **$p < 0.01$ when compared with the values from cells not exposed to an EF. Scale bars, 50 μm (B–D) and 25 μm (E). See also Figure S2 for experimental setup and electrotaxis response of NSCs from different species.

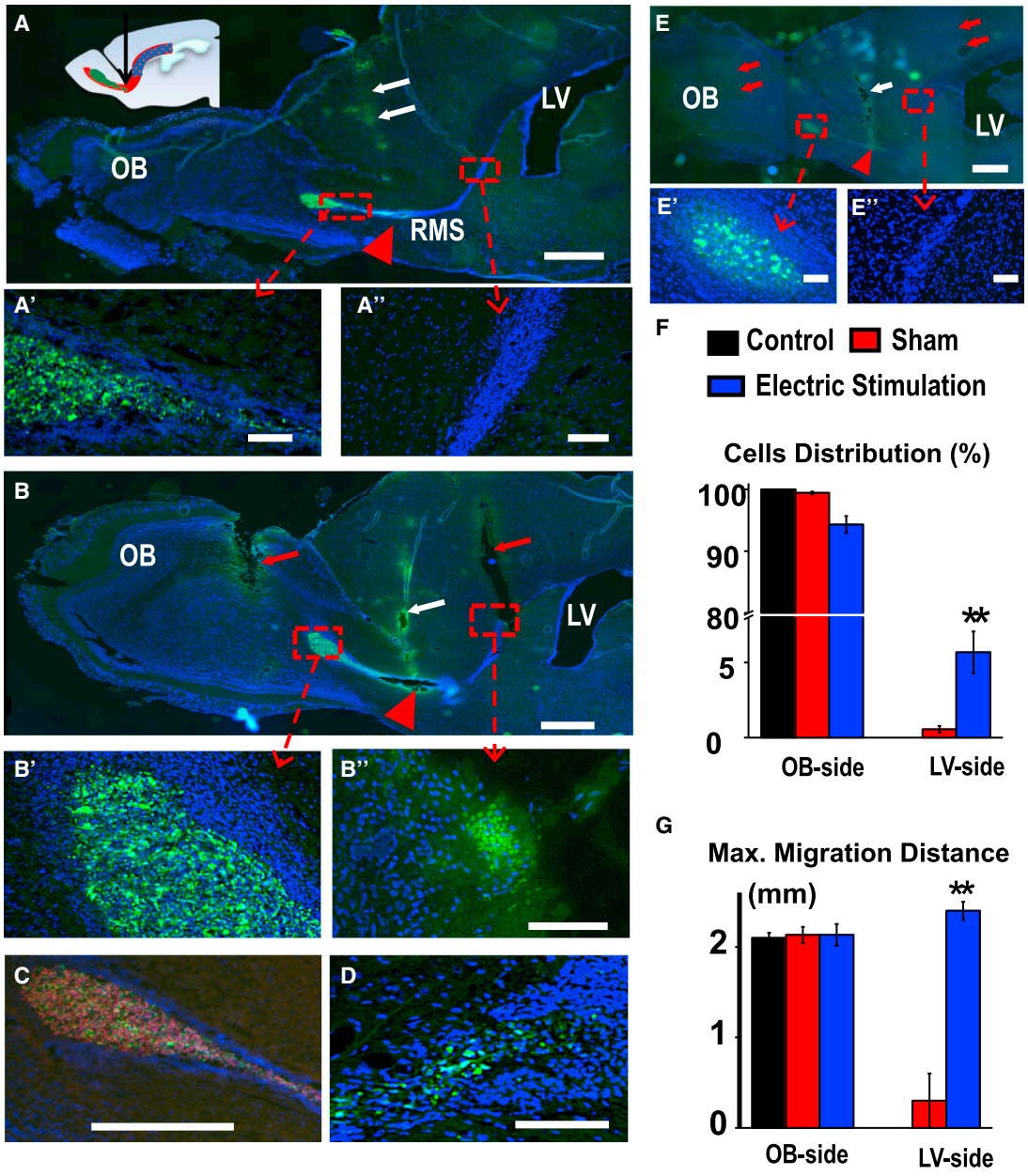

Figure 4. Electrical Stimulation Mobilized and Guided Migration of hNSCs in Rat Brain

(A) hNSCs transplanted into the middle part of rostral migration stream (RMS) had a default migration toward the olfactory bulb (OB). EGFP signals are evidently present on the OB side (A′), No EGFP signal was detectable on the lateral ventricle (LV) side (A″).

(B) Electrical stimulation (positive at OB and negative at LV side) induced significant amount of hNSCs to migrate to the LV side (B″) against co-existing guidance cues which normally guide cells to the OB side in the RMS. Larger number of hNSCs kept migration to the OB (B′). Electrodes were implanted and electrical stimulation was applied for 10 hr after 24 hr of EGFP-hNSC transplantation.

(C and D) Adjacent sections of the brain confirmed migration of hNSCs to the LV side.

(E) Sham stimulation, whereby stimulation electrodes were inserted without delivery of currents, showed no cell migration to the LV side (E″).

(F and G) Semi-quantification confirmed mobilizing and guidance effects of electrical stimulation. Electrical stimulation toward the SVZ guided a significant amount of hNSCs to the LV side, which was not seen in control groups. The maximum direct migration distance toward LV was 2.4 mm.

Means ± SEM from three independent experiments. **$p < 0.01$ versus electrode implant with no EF. Red arrowhead, cell transplant site; white arrow, injection needle path; red arrow, electrode insertion path. In (A) to (E″), DAPI is blue, EGFP green, and human SOX-2 red. Scale bars, 1 mm (A, B, and E), 500 μm (C), and 100 μm (A′, A″, B′, B″, D, E′, and E″).

the LV region and contralateral side suggests that the mobilizing effect of the electrical stimulation on hNSCs persisted even after the stimulation.

Using the transplant site as the middle point, we counted EGFP dots detected in the OB direction and that in the LV direction on the ipsilateral side, the sum being 100% (Figures 5B and 5C). Three weeks later, predominant signals of EGFP were in the LV region. Compared with the results immediately after electrical stimulation, more hNSCs were detected in the LV region than in the OB direction (compare Figure 5A with Figure 4A). Consistently, brains 4 months after stimulation showed an even greater proportion of hNSCs in the LV region (Figure 5C). The electrical stimulation not only guided cells to the SVZ, but the cells that traveled to in the LV region appeared to survive and maintain EGFP expression longer than the cells without stimulation.

We examined differentiation markers in hNSCs 3 weeks after transplantation and stimulation. No glial fibrillary acidic protein (GFAP) and neuron-specific class III β-tubulin (TUJ1) staining was found to co-localize with EGFP signals (Figure 6A). Four months after transplantation and stimulation, sparse EGFP signals could be shown to co-localize with antibodies against NEUN, GFAP, IBA1, and myelin basic protein (MBP), suggesting differentiation of some hNSCs to neuron, astrocytes, microglia, or oligodendrocytes (in CA1/CA2 region of hippocampus, in OB, in hippocampus, and in RMS, respectively.) (Figure 6B). These results are consistent with previous reports that transplanted hNSCs were able to differentiate in rodent brains (Flax et al., 1998; Tabar et al., 2005).

DISCUSSION

One unmet need in brain regenerative medicine is to effectively and safely mobilize and guide NSCs to migrate to the appropriate brain lesion sites for repair. Researchers have demonstrated the rich availability of NSCs both endogenously and through transplantation (Arvidsson et al., 2002; Bond et al., 2015; Gage, 2000). Inefficient migration, however, is one of the barriers to effective clinical use (Kornblum, 2007). For efficient treatment, transplanted stem cells must establish functional connections with the host cells to repair damage and restore function (Karp and Leng Teo, 2009; Khaldoyanidi, 2008; Laflamme and Murry, 2005). In most cases, very few stem cells are able to migrate to injured or diseased regions and integrate structurally and functionally in the well-differentiated host tissues (Rakic, 2004).

Our results demonstrated the feasibility of the application of electrical stimulation directly in the brain in a manner that stimulates and guides the migration of NSCs. Our optimized stimulation strategy and electrode system is able to deliver and monitor stable stimulation to the brain with minimized detrimental effects to a tolerable level, supported by assessment of EEG and motor function. In the RMS, where intrinsic signals normally guide NSCs toward the OB, the applied electrical signals were able to override the effect of intrinsic signals and guided some NSCs toward the SVZ. Significantly, electrical stimulation mobilized transplanted hNSCs to migrate beyond the attractive electrode to the SVZ and to a limited extent to the corpus callosum. hNSCs were found in the SVZ 3 weeks and 4 months after transplantation, long after EGFP signals disappeared in the OB. The hNSCs appeared to colonize some sites in the SVZ. Does this indicate that transplanted and electrically stimulated cells were able to replenish the stem cell reservoirs? We believe that this is a very important question to be answered in the future. A few transplanted cells appeared to start to express nerve cell markers, suggesting potential differentiation of those cells. The short-term guidance effects, and potential long-term motility increase and differentiation, suggest a useful aspect of electrical stimulation in brain function regulation through stem cells. We therefore provide proof-of-concept results to use electrical stimulation to guide and mobilize NSCs in the brain *in vivo*. One should note with caution that the RMS is a specific permissive area for neuronal migration in the adult brain. The microenvironment in injured brain is significantly different from that within the RMS. Future investigation is therefore essential to test subsequent hypotheses about the use of electrical stimulation to mobilize and guide migration of NSCs in diseased/injured brains.

Some neuroblasts migrate long distances from their place of origin to the resident destination throughout development and into adulthood (Altman, 1969; Alvarez-Buylla and Lim, 2004; Lois and Alvarez-Buylla, 1994; Luskin, 1993). Experiments using rodent models have produced significant insights into mechanisms that regulate NSC migration and show that chemical gradients are important guides in NSC migration (Aguirre et al., 2010; Duan et al., 2007; Famulski et al., 2010; Gaiano, 2008; Ishizuka et al., 2011; Li et al., 1999; McKay, 1997; Molnar and Clowry, 2012; Wang et al., 2011; Wu et al., 1999). Although powerful, chemical gradients are difficult to control *in vivo*. Application of EFs has flexibility of varying strength, time, and direction across long distances. The electric signal can be immediately switched on and off, and strength adjusted if so desired. Electrical guidance therefore may provide a useful approach in human brain, which is significantly larger—over a thousand times larger—than that of mouse or rat. EFs may be able to help to unify multiple cues in guiding cells as is currently being used in

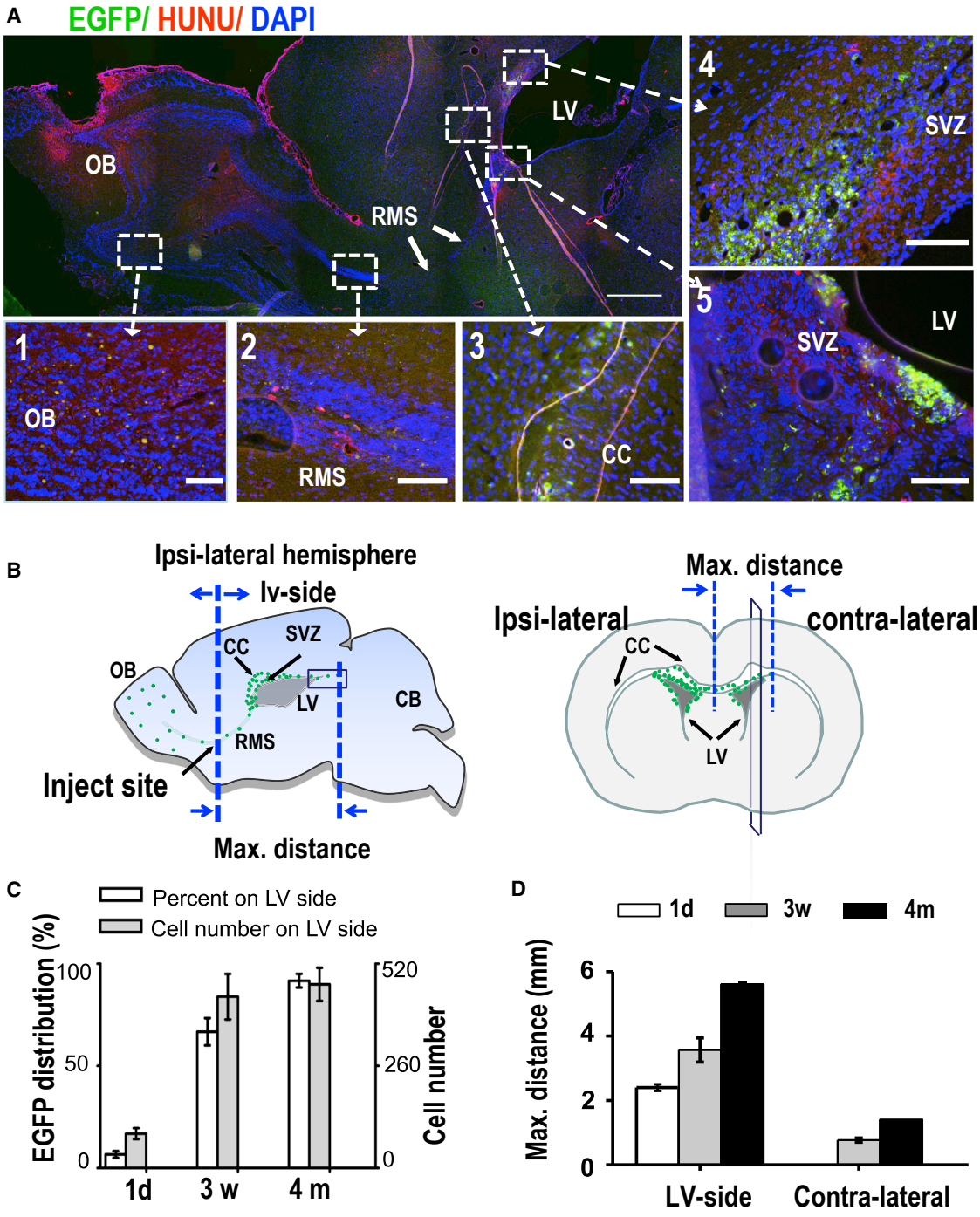

Figure 5. Electrically Guided Migration and Enhanced Motility of hNSCs in Rat Brain Persisted Long after Stimulation

(A) A typical sagittal section of a brain 3 weeks after electrical stimulation. EGFP signals are present in the OB and RMS. Co-labeling the cells with human nuclei antibodies (HUNU, red) confirmed human cell origin. hNSCs migrated beyond the stimulation electrode with majority of the cells appearing in the corpus callosum (CC) and the subventricular zone (SVZ) when comparing 1 and 2 with 3, 4, and 5. hNSCs appeared to have colonized in some regions of the SVZ.

(B) Diagrams illustrate assessment of distribution of hNSCs in the brain. EGFP signals 4 months post stimulation were assessed and are presented as green dots, showing cumulated distribution from serial sagittal sections, and coronal distribution of the cells from 3D

(legend continued on next page)

the treatment of epithelial migration in wound healing (Zhao et al., 2006). Further testing and optimization of electrical stimulation is needed in larger-brained animals and eventually in human brains. Development of stimulation technology in primates will lead to technology with promising clinical applications in human patients. Recent developments in deep brain stimulation technology and *in vivo* wearable electrode arrays suggest promising tools for regulation of function and structure of migrating hNSCs (Santhanam et al., 2006; Viventi et al., 2011).

EXPERIMENTAL PROCEDURES

Derivation of hNSCs and Establishment of EGFP-hNSCs

The use of human embryonic stem cells (hESCs) was approved by UC Davis Stem Cell Research Oversight Committee. hNSCs were derived from H9 hESCs as described in our previous publication (Feng et al., 2012a), then stably transduced with lentiviral vectors containing an EGFP reporter driven by the PGK promoter (EGFP-hNSCs). The confirmation of EGFP-hNSCs is described in Supplemental Experimental Procedures.

Electrotaxis of EGFP-hNSCs *In Vitro*

EGFP-hNSCs were seeded in an electrotaxis chamber in CO_2-independent medium (Invitrogen) plus 1 mM L-glutamine for 0.5–1 hr. Cell migration was recorded using time-lapse digital video-microscopy (Song et al., 2007). Directedness, migration speed, displacement speed, and x axis distance are the four parameters used to quantify cell migration, which are described in Supplemental Experimental Procedures.

Stimulation Schemes for Guidance of Cell Migration with Tolerable Detrimental Effects

To minimize the side effects of traditional continuous DC EFs, we optimized an intermittent DC EF stimulation scheme that effectively guides cell migration with minimal changes in temperature and pH. Additional information is provided in Supplemental Experimental Procedures.

Design of Electrodes for Implantation into the Brain *In Vivo*

Processed carbon rod and silver wire were used for current delivery electrode and the measuring electrode, respectively. The parameters and the electric circuit are described in Supplemental Experimental Procedures.

Design of a Programmable Stimulator to Deliver Electrical Stimulation *In Vivo*

We developed a programmable stimulator and fixed it on rat heads for stimulation *in vivo* with free movement of rats. Information in detail is provided in Supplemental Experimental Procedures.

Implantation of Electrodes in the Brain

The Institutional Animal Care and Use Committee at UC Davis approved all animal procedures in this study. Sprague-Dawley rats (Harlan, weighing 310–350 g) were used in the *in vivo* experiments. Animal preparation and care, and procedures of anesthesia and surgery are described in Supplemental Experimental Procedures.

Delivery of Electrical Stimulation to the Brain *In Vivo*

The electric circuitry was completed when the implanted electrodes were connected with the power supply or battery and voltmeter/ammeter, respectively. When electric current was delivered, real-time tissue currents, voltage, and resistance were recorded at indicated measuring positions. The animal grouping and observation for this section are described in Supplemental Experimental Procedures.

EEG During Electric Field Stimulation

Six rats were used for this part of the experiment. A level of anesthesia was maintained with ~1.5% isoflurane for minimizing the anesthetic effect on the EEG. The electrodes for electrical stimulation and recording, the positions of the electrodes, and the parameters applied in the EEG testing are described in Supplemental Experimental Procedures.

Transplant of EGFP-hNSCs and Animal Groups

EGFP-hNSCs were prepared at 50,000 cells/μL in NSC medium. At a speed of 1 μL/min, 5 μL of cell suspension was injected to the middle point of RMS (x = 3.7 mm, anterior from bregma; y = 1.2 mm, lateral from midline; z = −5.9 mm). A burr hole was then filled with bone wax and the scalp incision was sutured. Rats were placed into clean cages for recovery (one rat per cage post operation). After transplantation of cells, animals were randomly divided into three groups: control group (no electrodes implanted, n = 7), sham group (electrodes implanted with no electrical stimulation, n = 7), and electrical stimulation group (n = 10). For the long-term survival of rats, animal care was continued including observations of vocalizations, seizures, hemiplegic paralysis, and body weight. For sham-cell control, 5 μL of neurobasal medium with no cells was injected (n = 3, euthanized at 34 hr, 3 weeks, and 4 months post injection, respectively).

reconstruction form serial brain sections. Electrical stimulation mobilized cells not only to the LV (lv-side) in the injection hemisphere, but also into the contralateral hemisphere.

(C) Electrical stimulation increased distribution and the percentage of hNSCs to the LV side, which became more significant 3 weeks and 4 months after stimulation. Numbers of the EGFP cells in every brain section were increased on the LV side, especially in the SVZ. Means ± SEM from three independent experiments.

(D) Post-stimulation effects on the increased the migration distance on both the LV side and contralateral hemisphere. Means ± SEM from three independent experiments.

Scale bars, 1 mm (A) and 100 μm (A1–A6).

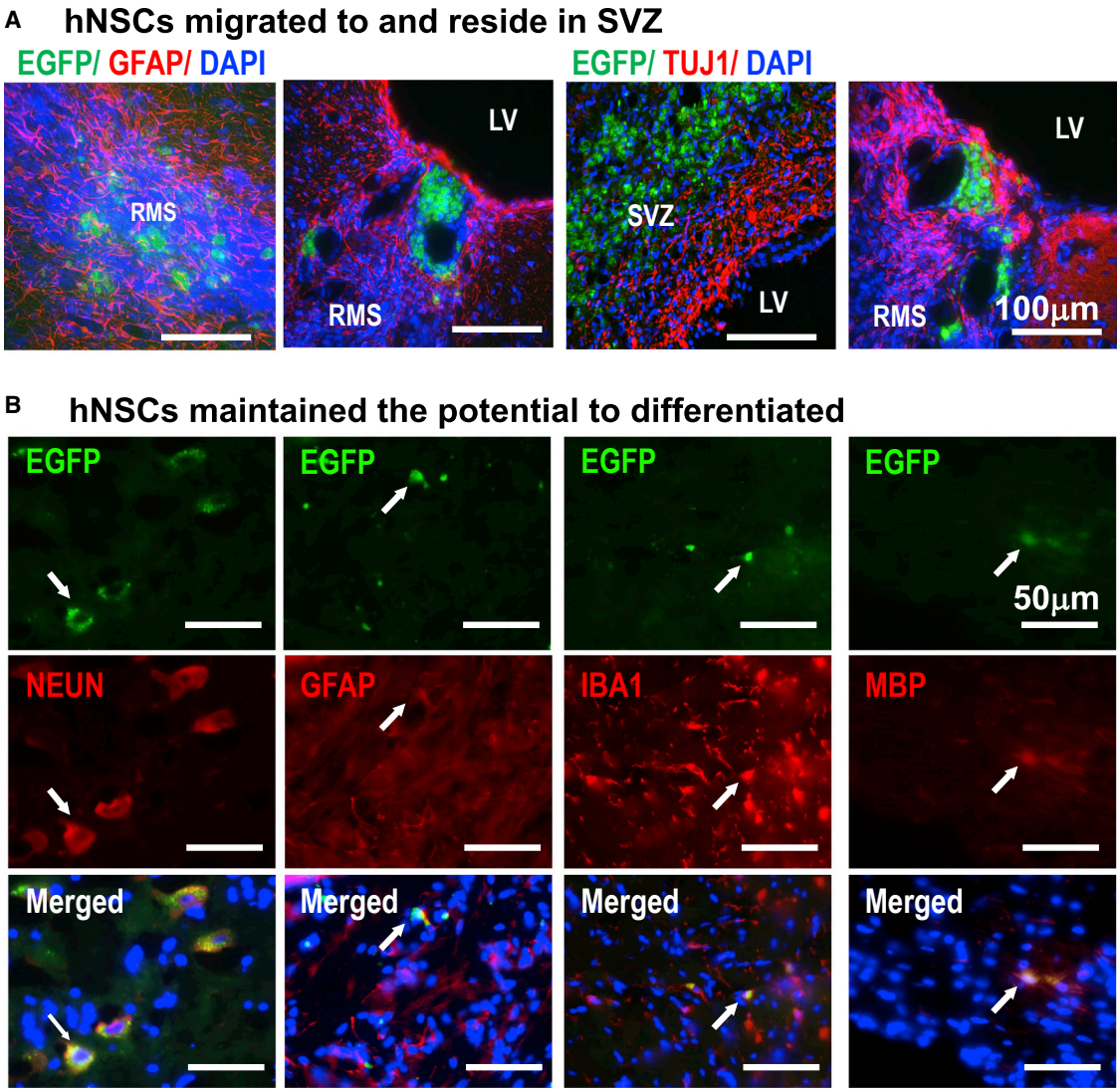

Figure 6. hNSCs Migrated over the Cathode Electrode and to the SVZ, which Appeared to Have the Ability to Differentiate

(A) EF stimulation reversed the migration of hNSCs to the SVZ. hNSCs resided in large area of the SVZ 3 weeks post EF stimulation. EGFP signals are mainly detected in the SVZ. The cells in green are not co-labeled red for either GFAP or TUJ1, indicating no differentiation to astrocyte or neuron of the graft cells.

(B) Four months after transplantation and electrical stimulation, hNSCs maintained EGFP. Co-localization of EGFP signals with NEUN (in CA1/CA2 region of hippocampus), GFAP (mainly in OB), IBA1 (in hippocampus), or MBP (found in RMS) (red) suggests possible differentiation of hNSCs to neuron, astrocyte, microglia, or oligodendrocyte, respectively.

All nuclei are labeled in blue with DAPI. White arrows show typical differentiated cells. hNSCs, human neural stem cells; SVZ, subventricular zone; EF, electric field; OB, olfactory bulb; RMS, rostral migration stream. Scale bars, 100 μm (A) and 50 μm (B).

Delivery of Electric Currents to Guide Migration of Transplanted EGFP-hNSCs

Twenty-four hours after cell transplantation, electrode implantation was performed. The output of power supply was adjusted for a target EF strength of 50–70 mV/mm during the 10-hr intermittent EF stimulation. Parameters were read from voltmeter, ohmmeter, and ammeter every 15 min. The animal grouping, animal care, and other information is provided in Supplemental Experimental Procedures.

Fixation of the Brain, Tissue Sectioning, and Immunohistochemistry

The procedure for the fixation of the brain and tissue sectioning is described in Supplemental Experimental Procedures. Brain sections were rehydrated and then blocked with blocking buffer containing 2% goat serum (Gibco), 1% BSA (Sigma), 0.1% cold fish skin gelatin (Sigma), 0.1% Triton X-100 (Sigma), and 0.05% Tween 20 (Sigma). Primary antibodies were incubated at room temperature for 1 hr followed by the application of second antibodies

(Alexa Fluor 594, Invitrogen). After washing with PBS, the tissue sections were mounted with an anti-fade mounting medium/DAPI mounting medium. The primary antibodies used were rabbit anti-human SOX2 (#3579, Cell Signaling Technologies, 1:200), mouse anti-human nuclei (#MAB1281, Millipore, 1:200), rabbit anti-GFAP (#AB5804, Millipore, 1:200), rabbit anti-TUJ1 (#ab24629, Abcam, 1:200), mouse anti-Neu-N (#MAB377, Millipore, 1:500), goat anti-IBA1 (#ab107159, Abcam, 1:1,000), and mouse anti-MBP (#ab24567, Abcam, 1:500).

Motor Functional Evaluation

Animals were trained to criteria on the behavioral tasks 2 days prior to cell transplantation, with the final day serving as the pre-surgery baseline. Electrical stimulation or controlled or sham interventions were applied 24 hr post cell transplantation. Animals were first tested on the Rotarod (Hamm et al., 1994) followed by horizontal ladder on post-electrical stimulation days 1, 4, 7, 11, and 15. Additional information for the Rotarod test and horizontal ladder-walk test are described in Supplemental Experimental Procedures.

Migration Analysis for EGFP Signals in Rat Brain

Brain sections were examined and analyzed with a fluorescent microscope system (Keyence, model BZ-9000 [BIOREVO]). For each individual rat brain, the center sagittal section was defined as most clearly showing the stem cell injection track and with the highest accumulation of EGFP signals. Two additional sections +16 μm and −16 μm away, respectively, were also selected for further detailed analysis. Thus three sections for each brain (hemisphere) were chosen for initial detailed analysis of cell migration. Additional information is provided in Supplemental Experimental Procedures.

SUPPLEMENTAL INFORMATION

Supplemental Information includes Supplemental Experimental Procedures, six figures, and three movies and can be found with this article online at http://dx.doi.org/10.1016/j.stemcr.2017.05.035.

AUTHOR CONTRIBUTIONS

J.-F.F. and M.Z. developed the conception, designed the study, analyzed and interpreted data, and wrote the manuscript, with help from all authors. J.-F.F. and J.L. collected and assembled most data. L.Z. assisted with cell culture and animal surgery. J.-Y.J. provided part of the study material. M.R., B.G.L., and J.N. were also involved in research design and provision of study materials. J.A.N. and M.Z. approved the final manuscript.

ACKNOWLEDGMENTS

This work is supported by grants from the California Institute of Regenerative Medicine RB1-01417 (to M.Z.) and TR1-01257 (to J.A.N.). M.Z. is also supported by NIH 1R01EY019101, NSF MCB-0951199, and UC Davis Dermatology Developmental Fund, and in part by the Research to Prevent Blindness. J.A.N. is also supported by the NIH (5P30AG010129, 5RC1AG036022-02, and 2P51RR000169-49). J.-F.F. is also supported by NSFC (31371406), STCSM (13ZR1424500), SMHS (XYQ2013094), and SMC-Star Award for Young Scholars (B). J.L. is supported by a fellowship from the Shriners of Northern California. J.-F.F., J.-Y.J., and M.Z. are also supported by MOST (2012CB518100). We thank Drs. Xian-Jiang Huang, Wei Liu, Natalie Grace, Michelle So, Lin Cao, Si-wei Zhao, Ken C. Van, Darrin Lee, and other members of the M.Z., B.G.L., and J.A.N. laboratories for assistance. M.Z. has research funding/contracted research with CIRM. M.Z., J.-F.F., and L.Z. are inventors of a US patent owned by UC Regents. M.R. does modeling of electrical current pathways with Aaken Laboratories.

Received: December 13, 2016
Revised: May 30, 2017
Accepted: May 31, 2017
Published: June 29, 2017

REFERENCES

Aguirre, A., Rubio, M.E., and Gallo, V. (2010). Notch and EGFR pathway interaction regulates neural stem cell number and self-renewal. Nature *467*, 323–327.

Altman, J. (1969). Autoradiographic and histological studies of postnatal neurogenesis. IV. Cell proliferation and migration in the anterior forebrain, with special reference to persisting neurogenesis in the olfactory bulb. J. Comp. Neurol. *137*, 433–457.

Alvarez-Buylla, A., and Lim, D.A. (2004). For the long run: maintaining germinal niches in the adult brain. Neuron *41*, 683–686.

Anton, E.S., Ghashghaei, H.T., Weber, J.L., McCann, C., Fischer, T.M., Cheung, I.D., Gassmann, M., Messing, A., Klein, R., Schwab, M.H., et al. (2004). Receptor tyrosine kinase ErbB4 modulates neuroblast migration and placement in the adult forebrain. Nat. Neurosci. *7*, 1319–1328.

Arvidsson, A., Collin, T., Kirik, D., Kokaia, Z., and Lindvall, O. (2002). Neuronal replacement from endogenous precursors in the adult brain after stroke. Nat. Med. *8*, 963–970.

Bond, A.M., Ming, G.L., and Song, H. (2015). Adult mammalian neural stem cells and neurogenesis: five decades later. Cell Stem Cell *17*, 385–395.

Cao, L., Wei, D., Reid, B., Zhao, S., Pu, J., Pan, T., Yamoah, E., and Zhao, M. (2013). Endogenous electric currents might guide rostral migration of neuroblasts. EMBO Rep. *14*, 184–190.

Curtis, M.A., Kam, M., Nannmark, U., Anderson, M.F., Axell, M.Z., Wikkelso, C., Holtas, S., van Roon-Mom, W.M., Bjork-Eriksson, T., Nordborg, C., et al. (2007). Human neuroblasts migrate to the olfactory bulb via a lateral ventricular extension. Science *315*, 1243–1249.

Duan, X., Chang, J.H., Ge, S., Faulkner, R.L., Kim, J.Y., Kitabatake, Y., Liu, X.B., Yang, C.H., Jordan, J.D., Ma, D.K., et al. (2007). Disrupted-In-Schizophrenia 1 regulates integration of newly generated neurons in the adult brain. Cell *130*, 1146–1158.

Famulski, J.K., Trivedi, N., Howell, D., Yang, Y., Tong, Y., Gilbertson, R., and Solecki, D.J. (2010). Siah regulation of Pard3A controls neuronal cell adhesion during germinal zone exit. Science *330*, 1834–1838.

Feng, J.F., Liu, J., Zhang, X.Z., Zhang, L., Jiang, J.Y., Nolta, J., and Zhao, M. (2012a). Guided migration of neural stem cells derived

from human embryonic stem cells by an electric field. Stem Cells *30*, 349–355.

Feng, J.F., Zhao, X., Gurkoff, G.G., Van, K.C., Shahlaie, K., and Lyeth, B.G. (2012b). Post-traumatic hypoxia exacerbates neuronal cell death in the hippocampus. J. Neurotrauma *29*, 1167–1179.

Flax, J.D., Aurora, S., Yang, C., Simonin, C., Wills, A.M., Billinghurst, L.L., Jendoubi, M., Sidman, R.L., Wolfe, J.H., Kim, S.U., et al. (1998). Engraftable human neural stem cells respond to developmental cues, replace neurons, and express foreign genes. Nat. Biotechnol. *16*, 1033–1039.

Gage, F.H. (2000). Mammalian neural stem cells. Science *287*, 1433–1438.

Gaiano, N. (2008). Strange bedfellows: Reelin and Notch signaling interact to regulate cell migration in the developing neocortex. Neuron *60*, 189–191.

Hamm, R.J., Pike, B.R., O'Dell, D.M., Lyeth, B.G., and Jenkins, L.W. (1994). The rotarod test: an evaluation of its effectiveness in assessing motor deficits following traumatic brain injury. J. Neurotrauma *11*, 187–196.

Ishizuka, K., Kamiya, A., Oh, E.C., Kanki, H., Seshadri, S., Robinson, J.F., Murdoch, H., Dunlop, A.J., Kubo, K., Furukori, K., et al. (2011). DISC1-dependent switch from progenitor proliferation to migration in the developing cortex. Nature *473*, 92–96.

Karp, J.M., and Leng Teo, G.S. (2009). Mesenchymal stem cell homing: the devil is in the details. Cell Stem Cell *4*, 206–216.

Khaldoyanidi, S. (2008). Directing stem cell homing. Cell Stem Cell *2*, 198–200.

Kornblum, H.I. (2007). Introduction to neural stem cells. Stroke *38*, 810–816.

Ladewig, J., Koch, P., and Brustle, O. (2014). Auto-attraction of neural precursors and their neuronal progeny impairs neuronal migration. Nat. Neurosci. *17*, 24–26.

Laflamme, M.A., and Murry, C.E. (2005). Regenerating the heart. Nat. Biotechnol. *23*, 845–856.

Li, H.S., Chen, J.H., Wu, W., Fagaly, T., Zhou, L., Yuan, W., Dupuis, S., Jiang, Z.H., Nash, W., Gick, C., et al. (1999). Vertebrate slit, a secreted ligand for the transmembrane protein roundabout, is a repellent for olfactory bulb axons. Cell *96*, 807–818.

Li, L., El-Hayek, Y.H., Liu, B., Chen, Y., Gomez, E., Wu, X., Ning, K., Li, L., Chang, N., Zhang, L., et al. (2008). Direct-current electrical field guides neuronal stem/progenitor cell migration. Stem Cells *26*, 2193–2200.

Lois, C., and Alvarez-Buylla, A. (1994). Long-distance neuronal migration in the adult mammalian brain. Science *264*, 1145–1148.

Luskin, M.B. (1993). Restricted proliferation and migration of postnatally generated neurons derived from the forebrain subventricular zone. Neuron *11*, 173–189.

McKay, R. (1997). Stem cells in the central nervous system. Science *276*, 66–71.

Meng, X., Arocena, M., Penninger, J., Gage, F.H., Zhao, M., and Song, B. (2011). PI3K mediated electrotaxis of embryonic and adult neural progenitor cells in the presence of growth factors. Exp. Neurol. *227*, 210–217.

Metz, G.A., and Whishaw, I.Q. (2002). Cortical and subcortical lesions impair skilled walking in the ladder rung walking test: a new task to evaluate fore- and hindlimb stepping, placing, and co-ordination. J. Neurosci. Methods *115*, 169–179.

Metz, G.A., and Whishaw, I.Q. (2009). The ladder rung walking task: a scoring system and its practical application. J. Vis. Exp. http://dx.doi.org/10.3791/1204.

Mobley, A.K., and McCarty, J.H. (2011). beta8 integrin is essential for neuroblast migration in the rostral migratory stream. Glia *59*, 1579–1587.

Molnar, Z., and Clowry, G. (2012). Cerebral cortical development in rodents and primates. Prog. Brain Res. *195*, 45–70.

Rakic, P. (2004). Neuroscience: immigration denied. Nature *427*, 685–686.

Sanai, N., Nguyen, T., Ihrie, R.A., Mirzadeh, Z., Tsai, H.H., Wong, M., Gupta, N., Berger, M.S., Huang, E., Garcia-Verdugo, J.M., et al. (2011). Corridors of migrating neurons in the human brain and their decline during infancy. Nature *478*, 382–386.

Santhanam, G., Ryu, S.I., Yu, B.M., Afshar, A., and Shenoy, K.V. (2006). A high-performance brain-computer interface. Nature *442*, 195–198.

Sawamoto, K., Wichterle, H., Gonzalez-Perez, O., Cholfin, J.A., Yamada, M., Spassky, N., Murcia, N.S., Garcia-Verdugo, J.M., Marin, O., Rubenstein, J.L., et al. (2006). New neurons follow the flow of cerebrospinal fluid in the adult brain. Science *311*, 629–632.

Snyder, E.Y., and Teng, Y.D. (2012). Stem cells and spinal cord repair. N Engl. J. Med. *366*, 1940–1942.

Song, B., Gu, Y., Pu, J., Reid, B., Zhao, Z., and Zhao, M. (2007). Application of direct current electric fields to cells and tissues in vitro and modulation of wound electric field in vivo. Nat. Protoc. *2*, 1479–1489.

Staquicini, F.I., Dias-Neto, E., Li, J., Snyder, E.Y., Sidman, R.L., Pasqualini, R., and Arap, W. (2009). Discovery of a functional protein complex of netrin-4, laminin gamma1 chain, and integrin alpha6beta1 in mouse neural stem cells. Proc. Natl. Acad. Sci. USA *106*, 2903–2908.

Stout, J.M., Knapp, A.N., Banz, W.J., Wallace, D.G., and Cheatwood, J.L. (2013). Subcutaneous daidzein administration enhances recovery of skilled ladder rung walking performance following stroke in rats. Behav. Brain Res. *256*, 428–431.

Tabar, V., Panagiotakos, G., Greenberg, E.D., Chan, B.K., Sadelain, M., Gutin, P.H., and Studer, L. (2005). Migration and differentiation of neural precursors derived from human embryonic stem cells in the rat brain. Nat. Biotechnol. *23*, 601–606.

Trounson, A., and McDonald, C. (2015). Stem cell therapies in clinical trials: progress and challenges. Cell Stem Cell *17*, 11–22.

Viventi, J., Kim, D.H., Vigeland, L., Frechette, E.S., Blanco, J.A., Kim, Y.S., Avrin, A.E., Tiruvadi, V.R., Hwang, S.W., Vanleer, A.C., et al. (2011). Flexible, foldable, actively multiplexed, high-density electrode array for mapping brain activity in vivo. Nat. Neurosci. *14*, 1599–1605.

Wang, Y., Kaneko, N., Asai, N., Enomoto, A., Isotani-Sakakibara, M., Kato, T., Asai, M., Murakumo, Y., Ota, H., Hikita, T., et al. (2011). Girdin is an intrinsic regulator of neuroblast chain migration in the

rostral migratory stream of the postnatal brain. J. Neurosci. *31*, 8109–8122.

Wu, W., Wong, K., Chen, J., Jiang, Z., Dupuis, S., Wu, J.Y., and Rao, Y. (1999). Directional guidance of neuronal migration in the olfactory system by the protein Slit. Nature *400*, 331–336.

Yao, L., Shanley, L., McCaig, C., and Zhao, M. (2008). Small applied electric fields guide migration of hippocampal neurons. J. Cell. Physiol. *216*, 527–535.

Yao, L., McCaig, C.D., and Zhao, M. (2009). Electrical signals polarize neuronal organelles, direct neuron migration, and orient cell division. Hippocampus *19*, 855–868.

Zhao, M., Song, B., Pu, J., Wada, T., Reid, B., Tai, G., Wang, F., Guo, A., Walczysko, P., Gu, Y., et al. (2006). Electrical signals control wound healing through phosphatidylinositol-3-OH kinase-gamma and PTEN. Nature *442*, 457–460.

Stem Cell Reports, Volume *9*

Supplemental Information

Electrical Guidance of Human Stem Cells in the Rat Brain

Jun-Feng Feng, Jing Liu, Lei Zhang, Ji-Yao Jiang, Michael Russell, Bruce G. Lyeth, Jan A. Nolta, and Min Zhao

Supplemental Figures 1-6

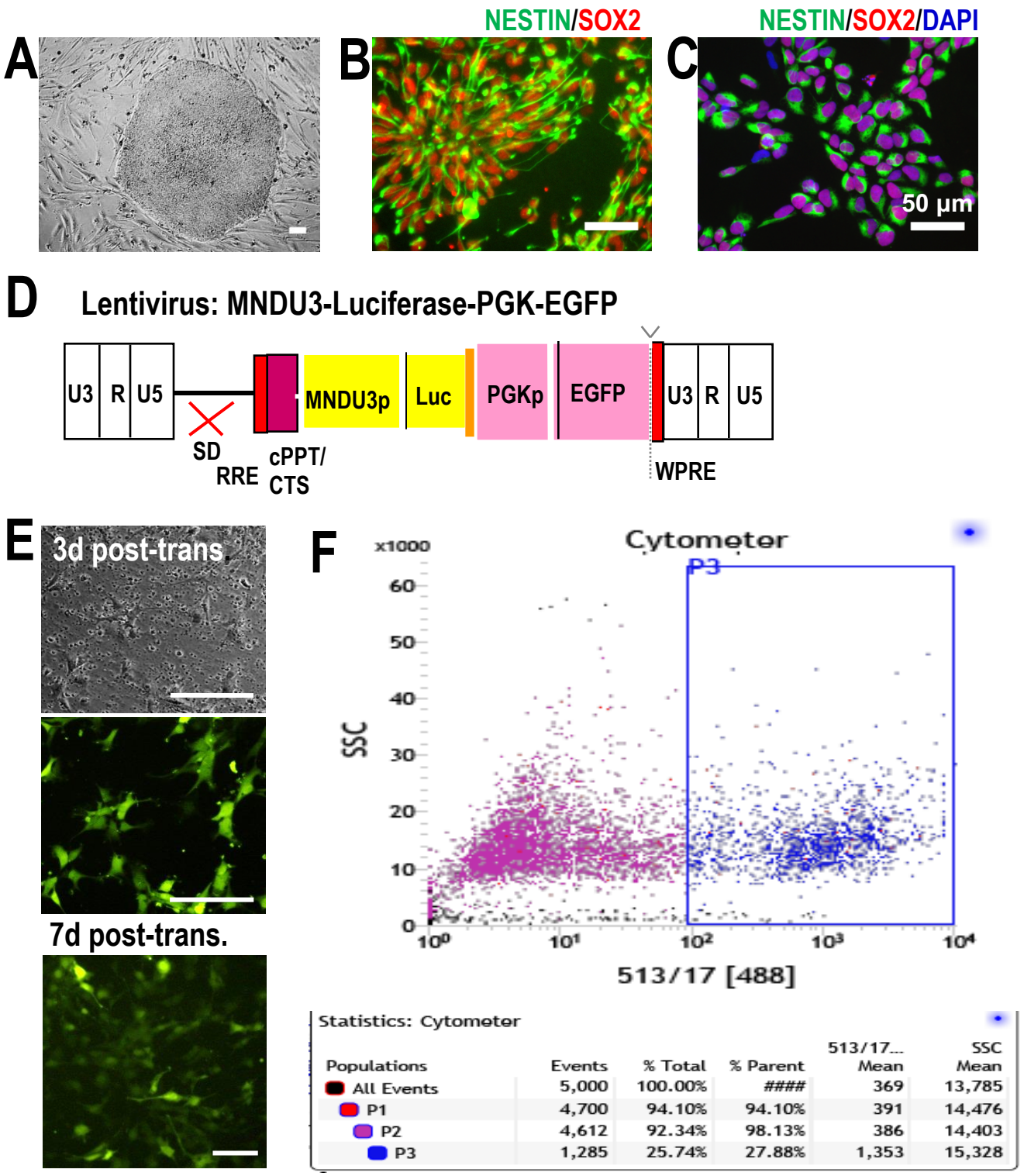

Figure S1. Derivation of human neural stem cells that express EGFP

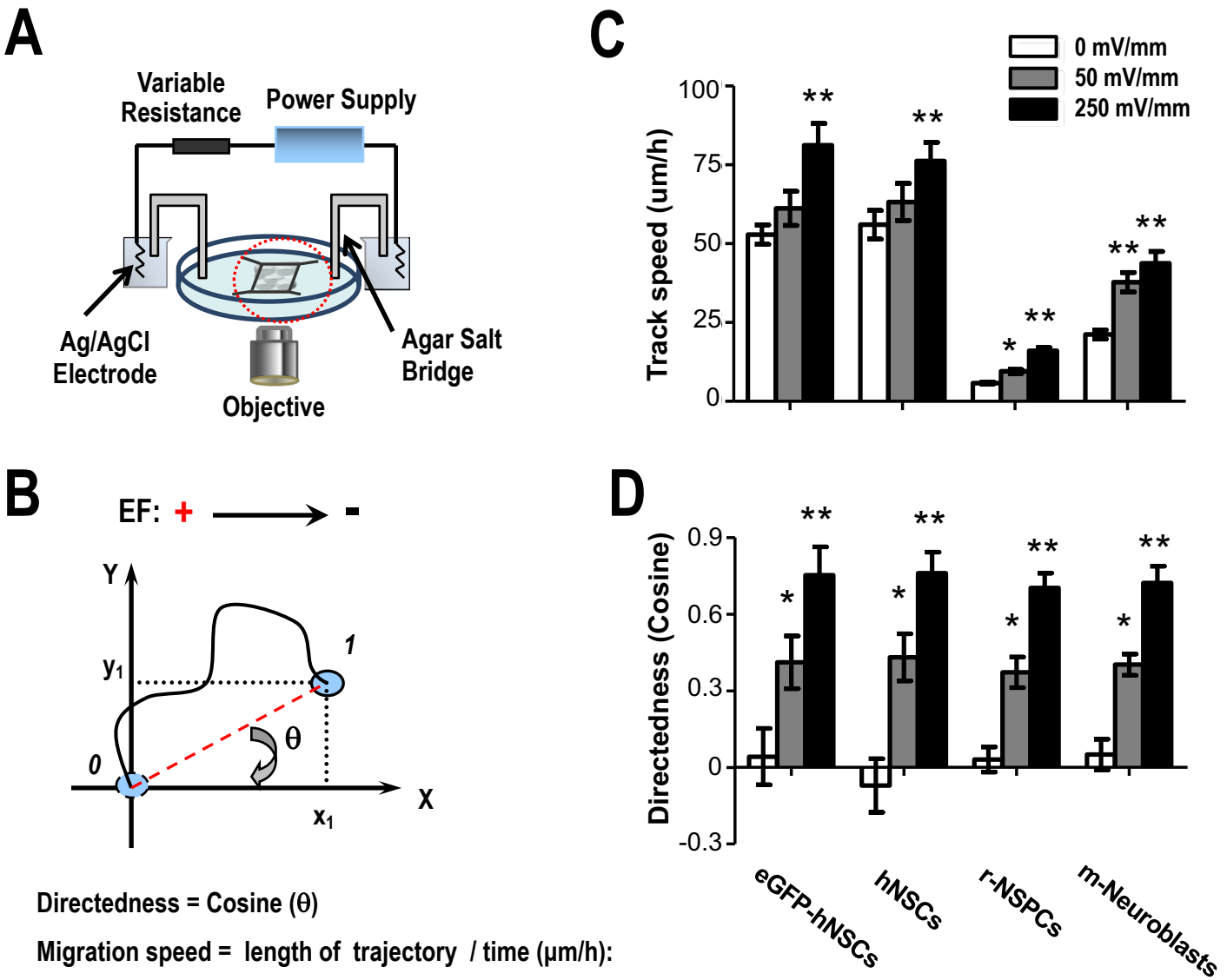

Directedness = Cosine (θ)

Migration speed = length of trajectory / time (μm/h):

Figure S2. ***In vitro*** **electrotaxis setup and investigation for different originated neuroblasts**

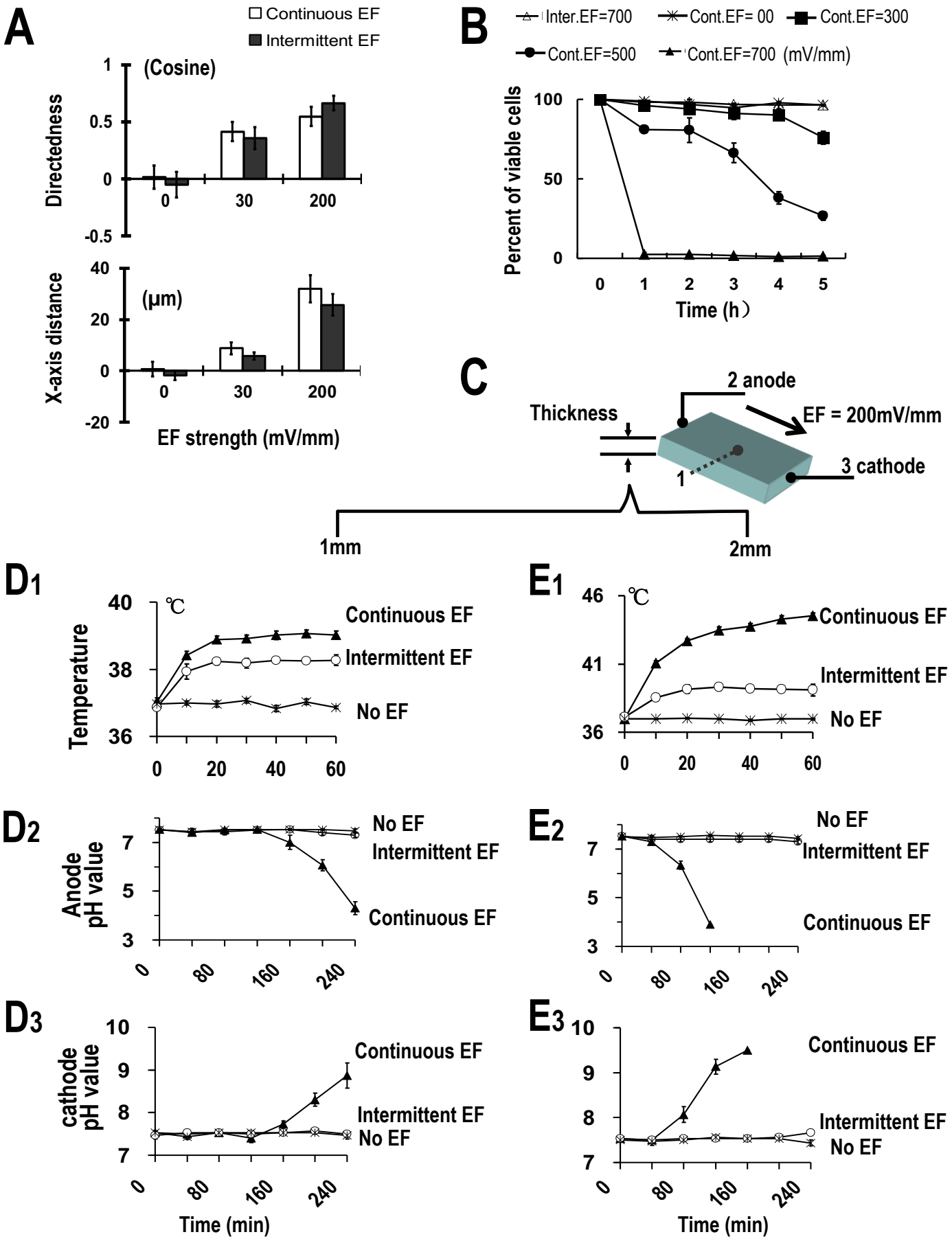

Figure S3. Intermittent EF stimulation guided migration of hNSCs with minimal cell damage and side effects

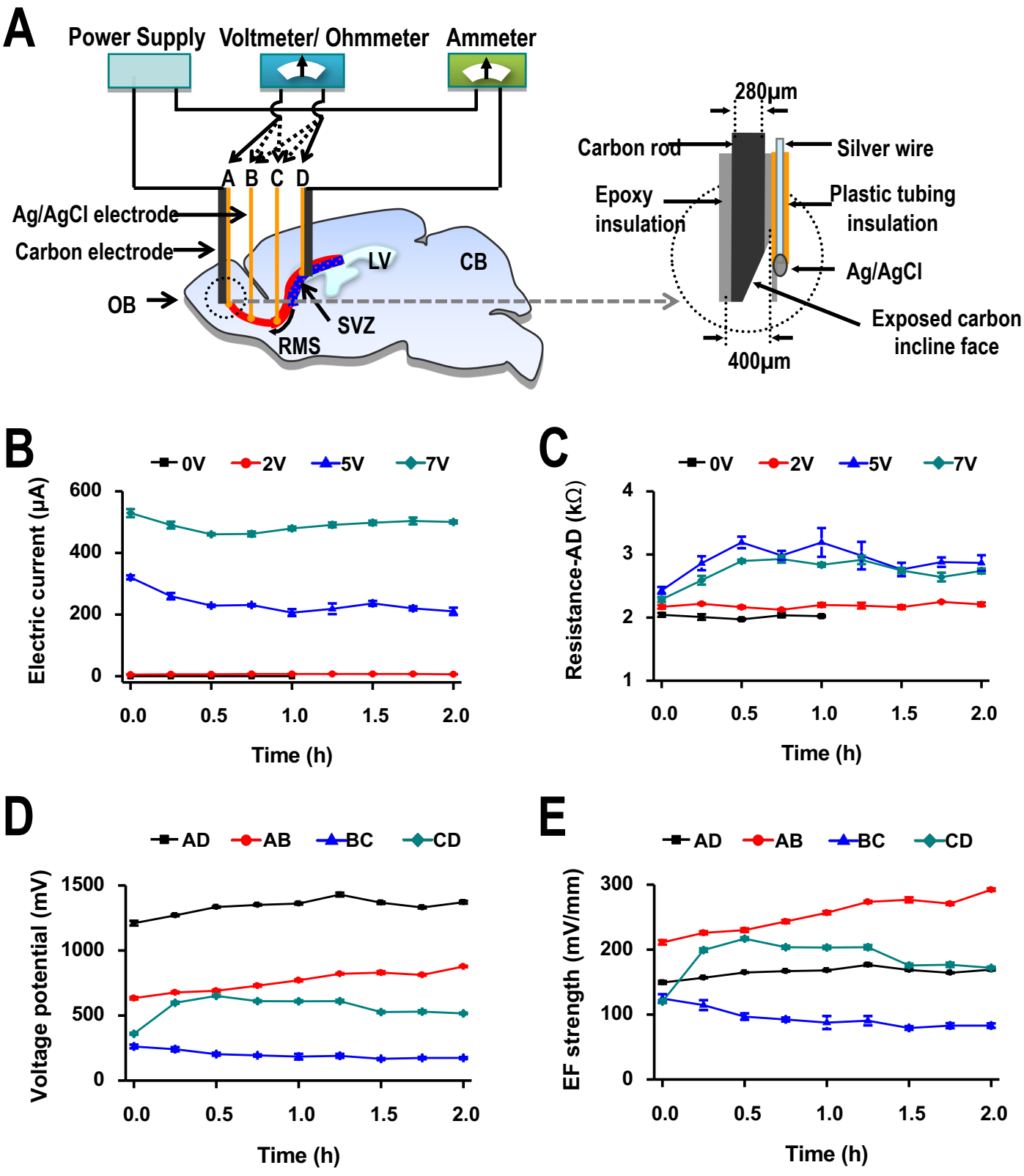

Figure S4. Electric fields and currents delivered which were stable in live animal brain

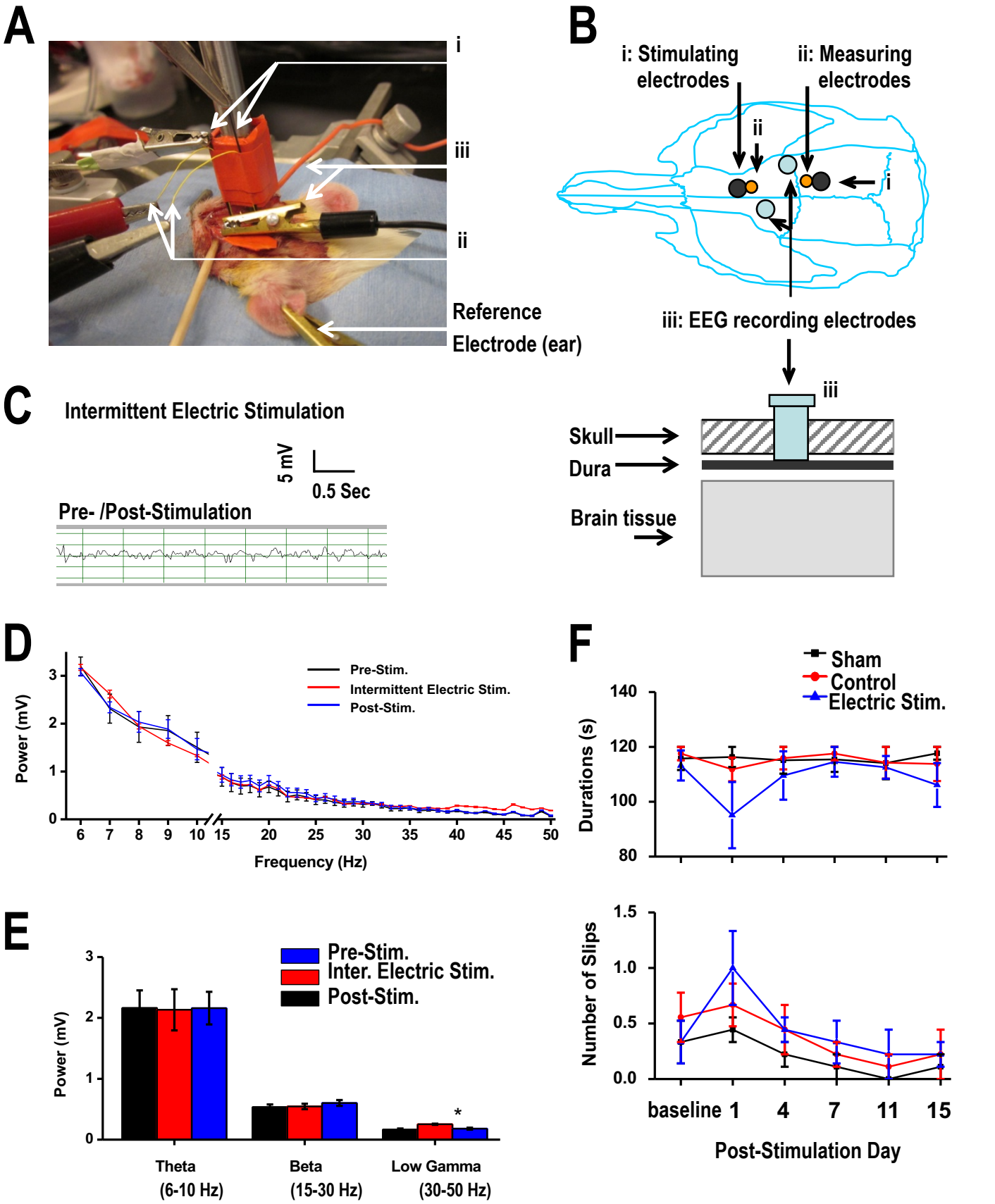

Figure S5. Electroencephalograph (EEG) monitoring during electrical stimulation and motor function evaluation after stimulation

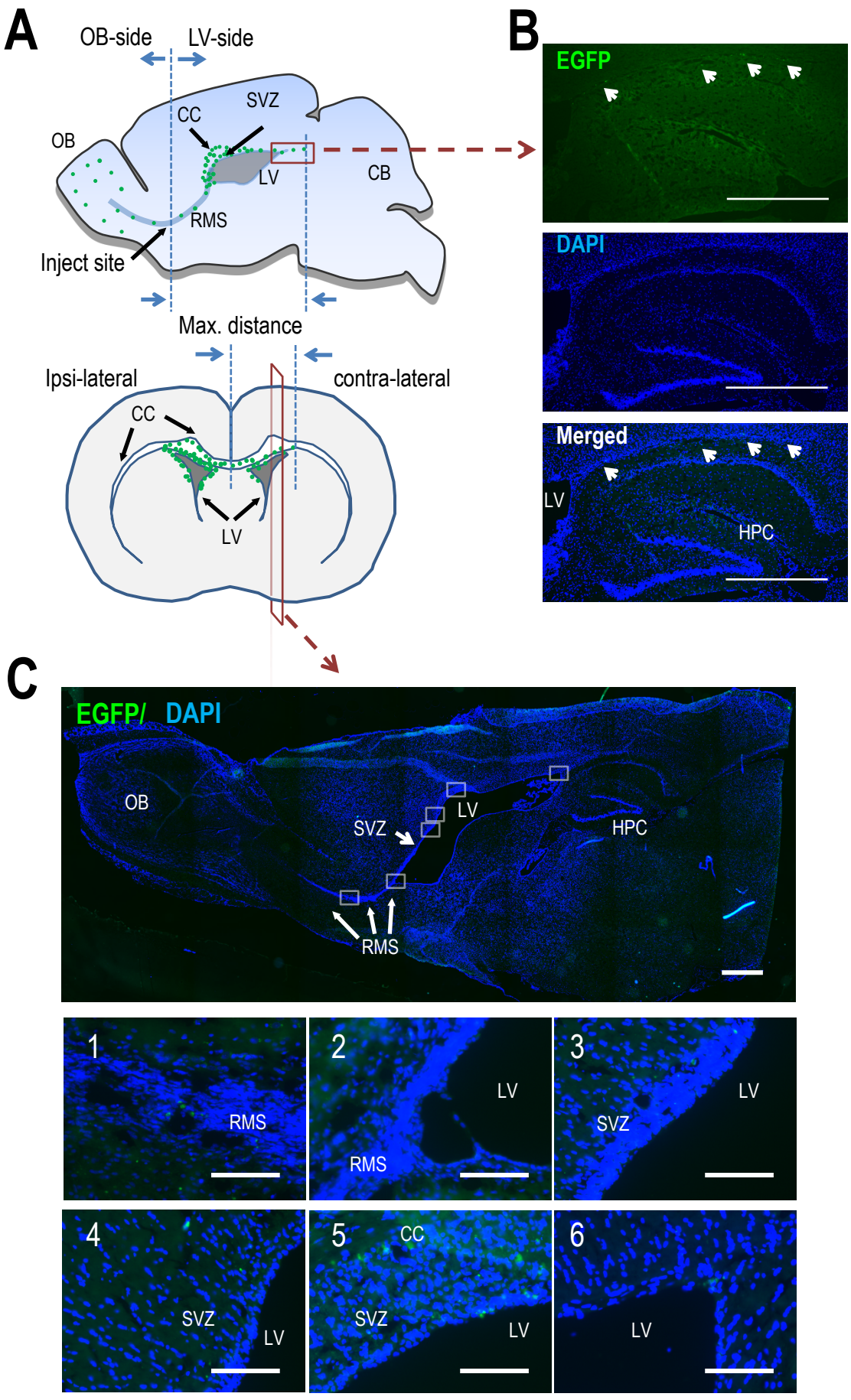

Figure S6. EGFP signals in lateral ventricle wall and the contralateral hemisphere

Legends for Supplemental Figures 1-6

Figure S1. Derivation of human neural stem cells that express EGFP

(A-C) Human embryonic stem cells cultured on feeder cells. The rosettes (B) and then the dissociated single human neural stem cells (hNSCs) (C) were positively labeled with anti-NESTIN and SOX2 antibodies.

(D) Lentivirus structure with the EGFP reporter.

(E-F) Transduction and expression of EGFP in hNSCs, and the enrichment of EGFP positive cells. EGFP: enhanced green fluorescence protein. Scale bar = 50 μm (A, B, C and E)

Figure S2. *In vitro* electrotaxis setup and investigation for different originated neuroblasts

(A) Experimental setup for *in vitro* electrotaxis assay. Cells were seeded in electrotaxis chamber, exposed to electric currents and migration behavior recorded with digital video microscopy.

(B) Cell migration is analyzed using migration speed and directedness value. An example of cell migration from the origin (0, 0) to (x_1, y_1).

(C, D) Electric fields significantly increased migration speed and guided migration of EGFP-hNSCs. (D) Galvanotaxis of EGFP-hNSCs in comparison to that of parental hNSCs, rat neural stem/progenitor cells (r-NSPCs) and mouse neuroblasts (m-neuroblasts).

Data are Means ± SEM from three or more independent experiments. $*P < 0.05$, $**P < 0.01$, when compared to cells not subjected an applied EF.

Figure S3. Intermittent EF stimulation guided migration of hNSCs with minimal cell damage and side effects

(A) Intermittent electric field (EF) stimulation achieved effective guidance the same as that induced in continuous EF stimulation on EGFP-hNSCs for 1 hr in an EF with strength indicated.

(B) Intermittent stimulation has evident advantage over continuous stimulation in that cell viability is significantly improved. Inter.: intermittent; Cont.: continuous. Data are presented as Means ± SEM from three or more independent experiments. Intermittent fields here shown were 1 sec on and 1 sec off.

(C) Measurement positions in an electrotaxis chamber with different chamber thickness to mimic volume conductive tissues. Electric field is as shown. The electrotaxis chamber used was of

dimension length (2.2 cm) and width (1 cm) with chamber thickness of 1 mm (D1-D3) or 2 mm (E1-E3). Data are presented as Means ± SEM from three or more independent experiments.
(D1, E1) Continuous stimulation induced significant changes in the temperature of the culture medium (measured at position 1). Intermittent stimulation reduced the change significantly.
(D2, E2) Continuous stimulation induced significant decrease in pH of the culture medium at the anode side, whereas intermittent stimulation completely prevented the changes.
(D3, E3) Continuous stimulation induced significant increased pH of the culture medium at the cathode side, whereas intermittent stimulation completely prevented the increase.

Figure S4. Electric fields and currents delivered which were stable in live animal brain
(A) Monitoring of the intermittent electrical stimulation in rat brain. Ag/AgCl electrodes at positions A, B, C and D to measure four positions along the RMS. Right panel is the schematic picture showing a carbon electrode and an Ag/AgCl electrode, for delivery and monitoring of the electric currents/fields. The electrodes were insulated with epoxy or plastic tubing and with the tips exposed.
(B) Stable electric currents recorded by the Ammeter.
(C) Electrical resistance between positions A and D. When 0 or 2 Volts of output was applied, the resistance value was registered directly on an ohmmeter between points A and D. When 5 or 7 Volts were applied, the resistance was deduced by R = V/I. R: resistance, V: voltage potential of AD, I: electric current value.
(D, E) The potentials at each point (D) and field strength (E) along the RMS when intermittent electric output was set at 7 Volts. Data are presented as Means ± SEM. In (B) and (C), each value at a single time-point was the mean of 3 values registered with 1-min time interval during the intermittent electrical stimulation (each from 1 rat). In (D) and (E), each value was the mean of 3 independent tests (each from 3 rats).

Figure S5. Electroencephalograph (EEG) monitoring during electrical stimulation and motor function evaluation after stimulation
(A) Various electrodes were implanted in an anesthetized rat.
(B) Schematic top view and lateral view illustrate the positions of stimulating electrodes (dark - i), measuring electrodes (yellow- ii), and EEG recording electrodes (blue - iii).

(C) Representative EEGs during intermittent electrical stimulation (1 sec on and 1 sec off as a cycle) at 4.4 V of output and that pre-/post stimulation.
(D-E) Frequency dependence of the power analysis of EEGs showed no changes in theta and beta waves. Low gamma wave increased however after stimulation. Data are presented as Means ± SEM from 3 rats. *$P < 0.05$ comparing to pre-stimulation.
(F) Motor function evaluation in rats with or without 10 hrs iEF stimulation post-transplantation. Rotarod (up) and Horizontal ladder-walk (down) tests showed no significant changes. Motor function appeared to be affected slightly in day 1 from the control group or sham group, but without significant statistic difference. From day 4 after stimulation, both tests showed the same motor functions between the experimental group, and the control and sham groups.

Figure S6. EGFP signals in lateral ventricle wall and the contralateral hemisphere
(A) Representative sagittal and re-constructed coronal brain sections. Green signals were detected in region close to hippocampus on the side with cell transplanted and the contralateral side of brain 4 months after electrical stimulation. Maximum distance is the distance from inject site to green signals farthest in ipsilateral hemisphere, and from the midline to farthest green signals on the contra lateral brain.
(B) EGFP signals are found far away from the inject site toward the hippocampus along the SVZ.
(C) EGFP signals are found on contralateral, distributed widely in CC, SVZ and RMS. Few green signals are co-labeled blue for DAPI.
Scale bar = 1000 μm (B and upper panel of C) or 100 (C1-6) μm. EGFP: enhanced green fluorescence protein, SVZ: subventricular zone, CC: corpus collosum, RMS: rostral migration stream.

Supplemental Experimental Procedures

1. Derivation of hNSCs and establishment of EGFP-hNSCs

Use of human embryonic stem cells was approved by UC Davis Stem Cell Research Oversight Committee. hNSCs were derived from H9 hESC as described in our previous publication *(Feng et al., 2012)*, then stably transduced with lentiviral vectors containing an EGFP reporter driven by the PGK promoter (EGFP-hNSCs). Cells were then enriched through cell sorting. Medium containing Glutamax, NEAA, N2 (1%), bFGF (20 ng/ml), 0.1% B27 and 10 ng/ml EGF on poly-l-ornithine/laminin coated dishes. To confirm the neural stem cell properties, cells were immunostained with NESTIN (MAB1259, R&D) and SOX-2 (#3579, Cell Signaling). EGFP- hNSCs were induced to differentiate into neurons and astrocytes as described previously and confirmed with staining of $EGFP^+/TUJ1^+$ or $EGFP^+/GFAP^+$ respectively *(Feng et al., 2012)* (Figures 2A-2D and Figure S1).

2. Electrotaxis of EGFP- hNSCs *in vitro*

EGFP-hNSCs were seeded in an electrotaxis chamber in CO_2 independent medium (Invitrogen) plus 1 mM L-Glutamine for 0.5-1 h. Cell migration was recorded using time lapse digital video-microscopy *(Song et al., 2007)* (Figure S2A). Following parameters were used to quantify cell migration: (1) Directedness was determined as the cosine (θ), where θ is the angle between the electric field vector and a straight line connecting the start and end position of a cell. A cell moving directly along the field lines toward the cathode (to the right) would have a directedness value of +1. A cell moving directly along the field lines toward the anode (to the left) would have a directedness value of -1. An average of cosine (θ) yields the directedness value for a population of cells, giving an objective quantification of the direction of cell migration. The cosine (θ) of a population of cells range from −1 to +1. A value close to 0 indicates cells migrate in random direction, whereas a value approaching +1 indicate guided migration of the cell population to the right (the cathode). (2) Migration speed (μm/h): accumulated migrated distance over time. (3) Displacement speed (μm/h): the straight line distance (in red) from the starting point to the final position of cell over time. (4) X-axis distance (μm): the distance which is projected on the X-axis (parallel to the electric field direction) from the starting point to the final position of cell's migration (Figure S2B).

3. Stimulation schemes for guidance of cell migration with tolerable detrimental effects

Continuous direct current (DC) electric fields can induce changes in temperature and pH in the culture medium, which are harmful to cells (Figure S3B). To minimize these effects, we optimized intermittent DC electric field stimulation scheme that effectively guide cells migration with minimal changes in temperature and pH. Temperature was recorded with a needle temperature probe (Physitemp unit TH-5, probe MT-29/2, Clifton, NJ) in the center of culture medium for 1 hr. pH values at both sides of the chamber were directly recorded for 4 hrs (Figures S3A, S3C-S3E3).

4. Design of electrodes for implantation into the brain *in vivo*

Carbon rod (Ø 280 μm) was used for current delivery electrode, with the tip exposed on a wedge face (30-40 degree) and other part insulated with epoxy. A silver wire insulated with plastic tubing (total Ø 200 μm) except the exposed tip of silver/ silver chlorides (Ag/AgCl) was used as the measuring electrode. The exposed tip was positioned in front of the carbon incline face (Figure 4A). The delivery and monitoring electrodes could be paired and implanted into brain tissues together to form a feedback-circuitry in brain tissue. An ammeter was used in the circuit for measuring the magnitude of electric current, a voltmeter connected to the Ag/AgCl electrodes for monitoring of voltage, and an ohmmeter for measuring the electric resistance. The output of power supply could be adjusted accordingly.

5. Design of a programmable stimulator for deliver electrical stimulation *in vivo*

We developed a programmable stimulator and fixed it on rat head for stimulation *in vivo* with rat free movement (Figure 3E). A 4 volts cell battery was assembled with a programed chip. The stimulation program was preset as 1 sec on and 1 sec off once the stimulation condition was initiated. When the stimulator was assembled to the carbon electrodes and electric circuit connected, the voltage potential tested from the carbon electrodes was 4 volts.

6. Implantation of electrodes in the brain

The Institutional Animal Care and Use Committee at the University of California at Davis approved all animal procedures in this study. Sprague-Dawley rats (Harlan, weighing 310–350 g) were used in the *in vivo* experiments. At least 7 days prior to surgery, animals were housed in individual cages in a temperature (22 °C) and humidity-controlled (50% relative) animal facility with unrestricted access to food and water and a 12 h light/dark cycle.

For surgery rats were anesthetized with 4% isoflurane in a carrier gas mixture of nitrous oxide/oxygen (2:1 ratio), intubated, and mechanically ventilated with a rodent volume ventilator (Harvard Apparatus model 683, Holliston, MA). A surgical level of anesthesia was maintained with 2% isoflurane. Rats were mounted in a stereotaxic frame, a scalp incision made along the midline, and four ~2 mm burr holes through the skull were performed on the right frontal and parietal bones (centered at X1=8.0, X2=5.0, X3=2.0, X4=-1.0 mm, anterior from bregma; and Y1=1.0, Y2=1.0, Y3=1.0, Y4=1.5 mm, lateral from mid-line, respectively). Dura was then carefully cut open under a surgical microscope. Two assembled carbon-Ag/AgCl electrodes and two single Ag/AgCl electrodes were arranged according to the four coordinates (X, Y as described at the center of four burr holes, Z1=-4.0, Z2=-6.0, Z3=-5.0, Z4=-4.0 mm, respectively) and fixed on a metal bar which clamped on the xyz-manipulator (Figure 3C). After alignment with Bregma via X, Y and Z controls, the metal bar lifted up slightly to locate the points of implant. Individual electrodes were adjusted slightly to avoid damaging cortical vessels. Electrodes were lowered and inserted into the brain tissue at a rate of 1 mm/min.

Following anesthesia, temporalis muscle temperature was monitored with a 29-gauge temperature probe (Physitemp unit TH-5, probe MT-29/2, Clifton, NJ) between the skull and temporalis muscle. Rectal temperature was monitored and maintained during surgical procedures by a feedback temperature controlled pad (CWE model TC-1000, Ardmore, PA).

7. Delivery of electric stimulation to the brain *in vivo*

The electric circuitry was completed when the implanted electrodes were connected with the power supply or battery and voltmeter/ammeter respectively. When electric current was delivered, actual in tissue currents, voltage and resistance were recorded at indicated measuring positions (Figure 1C and Figure S4A).

Ten rats were used to evaluate the electric delivery in brain *in vivo* (Figure S4). Animals were divided into three groups: three rats for continuous electric stimulation at 2, 5 or 7 volts for two hrs. Four rats for intermittent electric stimulation at strength of 0, 2, 5 or 7 volts, respectively (Figures S4B-S4C). The remaining three rats were used for measurements of electric fields at 7 volts of intermittent electric stimulation for two hrs (Figures S6D-S6E). Animals were observed for indications of seizures or abnormal activity during electric stimulation and during long-term

follow-up. Similar evaluation for the electric delivery in brain on the animals following transplantation of EGFP-hNSCs was performed (Figure 1D).

8. EEG during electric field stimulation

Six rats were used for this part of experiment. A level of anesthesia was maintained with ~1.5% isoflurane for minimizing anesthesia effect on EEG. The two assembled carbon-Ag/AgCl electrodes were used for electric stimulating and recording, positioned as previous described (X1=8.0, Y1=1.0, Z1=-4.0 mm, and X4=-1.0, Y4=1.5, Z4=-4.0 mm). Two skull screws (2.1mm diameter, 6.0 mm length) were placed into burr holes through the skull while keeping dura intact, 3 mm rostral to Bregma on left and 1 mm rostral to Bregma on right (see details in Figure S5A-S5B). In three rats, the screws were connected to EEG recording device (Grass Instruments model 7P5, Quincy, MA) for EEG recording pre-/ during/ post- intermittent DC electric field stimulation at 4.4 volts for 5 hrs using a programmable power supplier (Quadtech, 42006-300-8, CA). The other three rats experienced all the procedures except for electric stimulation. EEG data was filtered between 1 and 3kHz, digitized at 100 Hz, and stored on a computer. Frequency power analysis of EEG was measured using standard fast Fourier transform (Polyview 16 version 1.1 software; Grass Instruments, Quincy, MA).

9. Transplant of EGFP-hNSCs and animal groups

EGFP-hNSCs were prepared at 50,000 cells/μl in NSC medium. At a speed of 1ul/min, 5 ul cell suspension was injected to the middle point of RMS (X=3.7 mm, anterior from bregma; Y=1.2 mm, lateral from mid-line; Z= -5.9 mm). Burr hole was then filled with bone wax and scalp incision was sutured. Rats were placed into clean cages for recovery (1 rat/ cage post-operation).

After transplant of cells, animals were randomly divided into three groups: control group (no electrodes implant, n=7), sham group (electrodes implant with no electric stimulation, n=7) and electric stimulation group (n=10). For the rats of long-term survival, animal care was continued including the observation on vocalizations, seizures, hemiplegic paralysis and body weight. For sham-cell control, five μl neurobasal medium with no cells was injected (n=3, euthanized at 34 hrs, 3 weeks and 4 months post injection, respectively).

10. Delivery of electric currents to guide migration of transplanted EGFP-hNSCs

Twenty-four hours post cell transplant, electrode implantation was performed. The two assembled carbon-Ag/AgCl electrodes were used for electric stimulating and recording, positioned (X1=8.0, Y1=1.0, Z1=-4.0 mm, and X4=-1.0, Y4=1.5, Z4=-4.0 mm) (Figure 3D). Programmed power supply (Quadtech, 42006-300-8, CA) was connected to carbon electrodes and an ammeter for testing the electric current of the circuit. Ag/AgCl electrodes were connected to voltmeter and ohmmeter (Figure 1D). The output of power supply was adjusted for target electric field strength at 50-70 mV/mm during the 10 hrs' intermittent electric field stimulation. Parameters were read from voltmeter, ohmmeter and ammeter every 15 min.

Anesthesia was decreased to 1.5% isoflurane during intermittent electric field stimulation. Every 2 hrs, 1 ml saline was injected subcutaneously for fluid replacement. Saline was occasionally dropped on the burr holes to maintain moisture of brain tissue. In some groups with cell transplant, rats were euthanized immediately post stimulation (n=3), three weeks post stimulation (n=3) or four months post stimulation (n=1).

Another three rats in the electric stimulation group were fitted with the programmed stimulator and survived for two days before euthanization. Two carbon electrodes were implanted into rat brain (X1=8.0, Y1=1.0, Z1=-4.0 mm, and X4=-1.0, Y4=1.5, Z4=-4.0 mm) (Figure 3E). When the programmed stimulator was connected and fixed to the carbon electrodes, paraffin was used to seal the stimulator in a plastic cover which was secured over the exposed skull with cyanoacrylate glue. Animal care was continued including observation of vocalizations, seizures, hemiplegic paralysis and body weight until time of euthanasia.

11. Fixation of the brain, tissue section and immunohistochemistry

Rats were euthanized by injection of sodium pentobarbital (100 mg/kg, ip), followed by transcardial perfusion with 100 ml of 0.1 M sodium phosphate buffer (PB) (pH=7.4), then perfusion fixation with 300 ml of 4% paraformaldehyde at 4 °C (pH=7.4). Brains were removed and additionally fixed for 1 hr. in 4% paraformaldehyde at 4°C. Brains were cryoprotected in 10% sucrose solution for 1 day followed by 2 days in a 30% sucrose solution, embedded with optimal cutting temperature compound (O.C.T. Compound, Tissue-Tek), and 8 um sagittal sections were cut on a freezing cryostat. Sections were stored at -80°C before immunohistochemistry.

Brain sections were rehydrated in phosphate buffered saline (PBS) for 10min and then blocked with the blocking buffer containing 2% goat serum (Gibco), 1% BSA (Sigma), 0.1%

cold fish skin gelatin (Sigma), 0.1% Triton X-100 (Sigma) and 0.05% Tween 20 (Sigma). Primary antibodies were incubated at room temperature for one hour followed by the application of second antibodies (Alexa Fluor 594 nm, Invitrogen). After washing with PBS, the tissue sections were mounted with an anti-fade mounting media/DAPI mounting media. The primary antibodies used were rabbit anti- human SOX2 (#3579, Cell Signaling, 1:200); mouse anti-human Nuclei (MAB1281, Millipore, 1:200); rabbit anti- GFAP (AB5804, Millipore, 1:200); rabbit anti-TUJ1 (ab24629, Abcam, 1:200); mouse anti- Neu-N (MAB377, Millipore,1:500); Goat anti-IBA1 (ab107159, Abcam, 1:1000); Mouse anti-MBP (ab24567, Abcam, 1:500).

12. Motor functional evaluation

Animals were trained to criterion on the behavioral tasks two days prior to cell transplant, with the final day serving as the pre-surgery baseline. Electric stimulation or controlled or sham interventions were applied 24 hours post cell transplant. Animals were first tested on the rotarod followed by horizontal ladder on post electric stimulation days 1, 4, 7, 11, and 15.

Rotarod test

Duration that the animals could maintain ambulatory activity on the rotarod was measured to evaluate coordination, balance, and endurance by trained personnel blinded to the identity of the animal groups as previously described *(Hamm et al., 1994)*. Animals were placed on a 4-lane rotarod (Ugo Basile model 7700; Comerio, Italy) with a constant speed (12 rpm, 3.6 cm/sec). 120 sec was the maximum time allowed on the rotarod. Rats were tested three times on each testing day, with a 5 min rest period in between trials, and the mean latency of three trials was calculated for each animal.

Horizontal ladder-walk test

Fine motor coordination was assessed with the ladder-walk test. Rats were trained to walk across an elevated, horizontal, level ladder 1.1m length X 10cm width. This ladder was bounded between 20cm high transparent Plexiglas walls on both sides. The ladder steps consisted of 2.5mm diameter rungs, with 1.25cm spaces between them. The rats were trained to escape from an aversive auditory stimulus by walking across the ladder in order to enter a goal box at the opposite end. The noise was terminated when the rat entered the goal box at the opposite end of the ladder. The test consisted of 3 such trials. Rats remained in the escape box for 15 sec after

each trial. The number of "slips" in which a leg extended down through the rungs without grasping the rung was counted. The total time required for the rat to traverse the ladder was also recorded. The rats were trained on the ladder for 2 days before the electrical stimulation and then baseline was recorded prior to the surgery on the day of the electrical stimulation. The test was performed on days 1, 4, 7, 11 and 15 post electrical stimulation. Each trial was recorded using a video camera for later scoring and analysis.

13. Migration analysis for EGFP signals in rat brain

Brain sections were examined and analyzed with a fluorescent microscope system (Keyence, model BZ-9000 (BIOREVO); Itasca, Il). For each individual rat brain, the center sagittal section was defined as most clearly showing the stem cell injection track and with the highest accumulation of EGFP signals. Two additional sections which was +16um and -16um away respectively were also selected for further detailed analysis. Thus 3 sections for each brain (hemisphere) were chosen for initial detailed analysis of cell migration.

For the animals euthanized immediately post electric stimulation (n=3 for each group - control, sham and electric stimulation), semi-quantification was performed to assess the EGFP-cells distribution. In each section, all the EGFP positive cells on both OB- and LV-region were counted as 100%. The percent of EGFP positive cells on LV-region was detailed defined based on the cell number: 0% ~ no signals (< 5/section), 1% ~ find very few scattered green signals (< 10/section), 5% ~ (<100/section), 10% ~ (>200/section). Furthermore, the EGFP positive cells number in each brain section was counted under microscope individually. The maximum migration distance was obtained directly under the microscope for each section on both regions. If the maximum distance was within 200um from inject site, we considered as no migration. For the animals euthanized three weeks post stimulation (n=3 for each group) and four months post stimulation (n=1 for each group), the same analysis was performed for EGFP percent on LV-region and maximum distance on LV-region. The contra-lateral hemisphere of these rats were also cut and reserved as sagittal sections, for assessing the EGFP migration on contra-lateral (Figure S6C). Since only 1 rat/ group in the four-months survival group, fifteen sections were analyzed from each rat (3 sections for each primary cellular antibody NEUN, GFAP, IBA 1, MBP, and 3 for control) rather than 3 sections.

REFERENCES

Feng, J.F., Liu, J., Zhang, X.Z., Zhang, L., Jiang, J.Y., Nolta, J., and Zhao, M. (2012). Guided migration of neural stem cells derived from human embryonic stem cells by an electric field. Stem cells *30*, 349-355.

Hamm, R.J., Pike, B.R., O'Dell, D.M., Lyeth, B.G., and Jenkins, L.W. (1994). The rotarod test: an evaluation of its effectiveness in assessing motor deficits following traumatic brain injury. Journal of neurotrauma *11*, 187-196.

Song, B., Gu, Y., Pu, J., Reid, B., Zhao, Z., and Zhao, M. (2007). Application of direct current electric fields to cells and tissues in vitro and modulation of wound electric field in vivo. Nature protocols *2*, 1479-1489.

Supplementary Videos legends

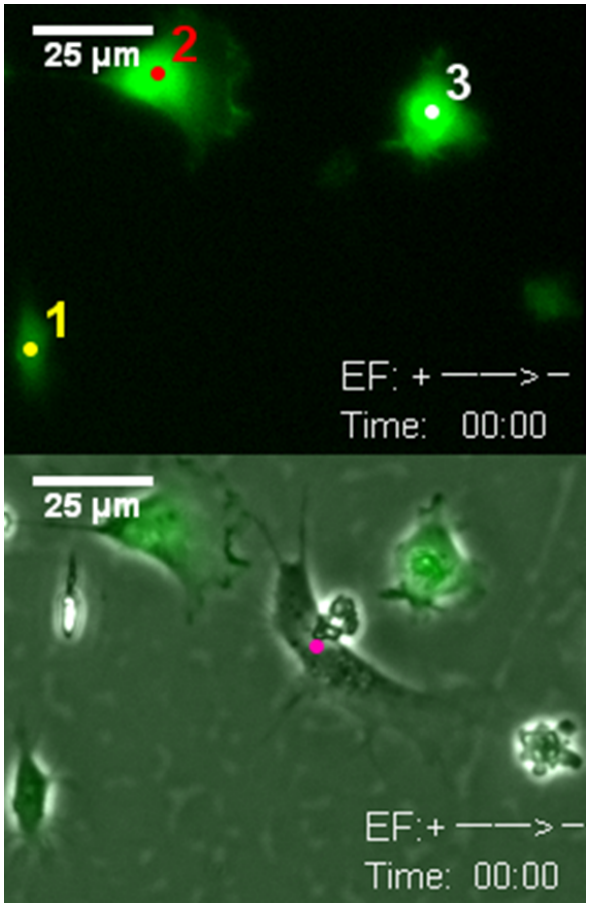

Video S1. EGFP-hNSCs showed robust cathodal migration in EF as that of non-transfected hNSCs

Upper panel: EGFP positive hNSCs shown in GFP channel. Lower panel: Merged video shows EGFP positive and negative hNSCs in the same electric field (EF). Cells with EGFP migrate as robust as the cells not transfected with EGFP. Cells migrated directionally to the cathode in the first 100 min and then migrated to the new cathode after the reversal of EF in the second 100 min. EF = 250 mV/mm. Polarity, time (hour: min) and scale are indicated. EGFP: enhanced green fluorescence protein, hNSCs: human neural stem cells.

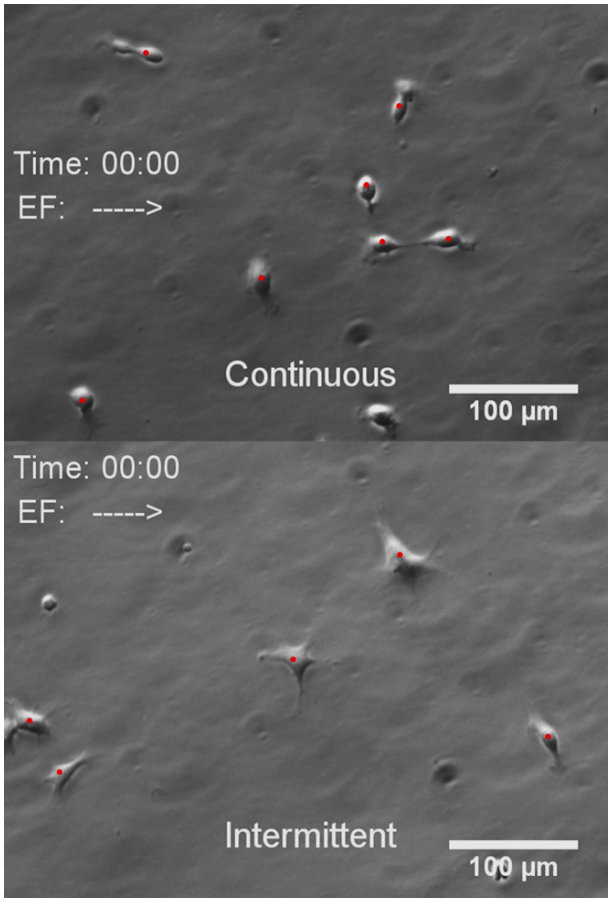

Video S2. Electrotaxis of hNSCs in continuous and intermittent direct current EFs

Robust cathodal migration of hNSCs in both continuous (upper panel) and intermittent (lower panel) direct current EFs. EF = 200mV/mm. Polarity, time (hour: min) and scale as shown. hNSCs: human neural stem cells; EF: electric field.

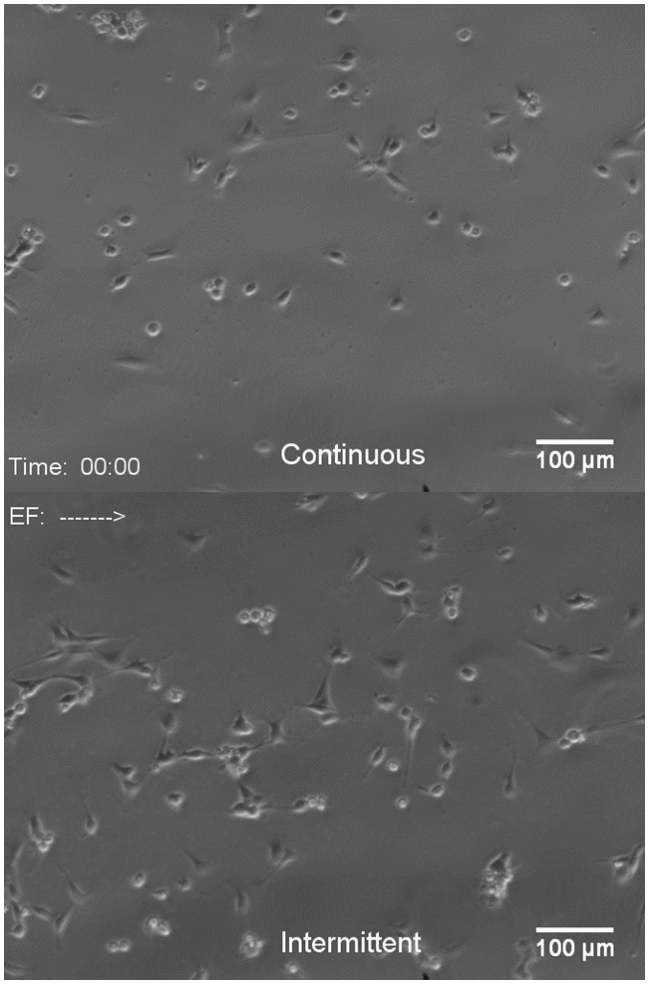

Video S3. Safety advantage of intermittent EF stimulation over continuous EF stimulation

In an intermittent EF (lower panel), cells survived, whereas died rapidly in continuous EF stimulation (upper panel). EF = 700 mV/mm. Polarity, time (hour: min) and scale as shown. EF: electric field.